ADAPTIVE MODULATION TECHNIQUES FOR BANDWIDTH AND POWER EFFICIENT COMMUNICATION

Muhammad Kaleem Munawwar Khodabacchas

Master Of Research

Department of Electronic Engineering
Macquarie University

October 09, 2015

Supervisor: Associate Professor Sam Reisenfeld

ACKNOWLEDGMENTS

I would like to acknowledge Associate Professor Sam Reisenfeld for the constant support, guidance and for the hours spent answering my questions patiently and helped me understand this area in depth. I would also like to thank Professor N.Balakrishan and Professor M.V Koultras for their suggestions regarding the number of available adjacent channel pairs. I also would like to thank my parents and family for always being there for support, and finally I would also extend my thanks to my friends and classmates who were always there whenever a quick advice or help was needed.

STATEMENT OF CANDIDATE

I, Muhammad Kaleem Munawwar Khodabacchas, declare that this report, submitted as part of the requirement for the award of Bachelor of Engineering in the Department of Electronic Engineering, Macquarie University, is entirely my own work unless otherwise referenced or acknowledged. This document has not been submitted for qualification or assessment an any academic institution.

Student's Name: Muhammad Kaleem Munawwar Khodabacchas

Student's Signature: M K M Khodabacchas

Date: 09 Oct 2015

ABSTRACT

Cognitive Radio (CR) describes a system which adapts to the environment in which it is operating and adjusts to its radio operating parameters dynamically and autonomously. It also learns from the actions undertook and its subsequent responses in the current environment. Progress in the field of radio technology enabled radios to manage their power, time and bandwidth resources in order to make best possible use of available spectrum. This project investigates how, when given a spectrum opportunity, one can transmit at lower possible power level that still maintains adequate secondary user Bit Error Rate (BER) performance. The bandwidth availability in cognitive radio dynamically change, and therefore adaptive modulation techniques may be used to most effectively utilise available bandwidth, while minimising interference to primary users. Moreover, techniques for monitoring the Signal-to-Noise ratio (SNR), Eb/No, and for adapting the modulation are also investigated. Analytical methods and digital communication systems simulations are devised. In addition, the performances of adaptive systems are presented. Furthermore, the performance results were obtained for adaptive systems transmitting over a Jakes model, Rayleigh Fading Channel. Both cases of very fast and slow fading Rayleigh channel and adapting to the changes in average SNR, Eb/No, therein are investigated.

Contents

Chapter 1

Introduction

Due to unprecedented advances in wireless access technologies and the proliferation of wireless devices and applications, there is a major change in wireless network traffic. Recently, a study done by Cisco [1], wireless data is predicted to grow exponentially. More precisely, by the end of 2014, the number of mobile-connected devices will be exceeding the number of people on earth, and by 2019 there will be nearly 1.5 mobile devices per capita. A study of the New American Foundation with the cooperation of the Shared Spectrum Company to find the extent to which the spectrum is currently being utilised. The outcome, which is measurements in the 30-300MHz band, demonstrates that the usage of some radio channels is less than one percent, while the mean occupancy over all the frequency bands is a meagre 5.2 percent. We can hence, deduce that dividing spectrum into blocks in not efficient and this way of rigid allocation policies have given rise to an artificial scarcity of radio resources [2]. Such fundamental changes in wireless data volume and composition bring about great challenges for the design and operation of wireless access networks. The capacity of existing and future wireless networks will be greatly stressed. Although allocating more spectrum may help, we are facing the problem of spectrum depletion since it is not a regenerable resource. Improving spectrum efficiency thus becomes ultimately important. Among the potential techniques, Cognitive radio (CR) is an effective solution to meet the critical demand in wireless network capacity. With knowledge of their RF local environment, CR can enhance the link reliability and help wireless systems improve coverage and capacity. In his paper, Joseph Mitola coined the term CR as a way to efficiently use the underutilised frequency spectrum [3] and how CR can greatly improve the flexibility of personal wireless services through Radio Knowledge Representation Language (RKRL). Although considerable foray have been made and insights have been gained in various aspects of CR, the problem of guaranteeing application performance [4] has not been in the limelight of CR research. In the same breath, in most spectrum sensing schemes, dynamics of the channel in a fading environment have not been fully addressed [5], thus leading to inefficient spectrum utilisation. This thesis will place particular focus on the concepts of adaptive modulation and how it can be used in CR to maximise the spectrum efficiency of wireless communication. The main aim of the project is to investigate how, when a spectrum slot becomes available,

one can transmit at lowest possible level that still maintains adequate BER performance. Given the bandwidth availability in CR dynamically change, using adaptive modulation techniques can be used to advantage to utilise the bandwidth as efficiently as possible, while keeping interference to PUs to a minimum. Conventional wireless communication systems based upon fixed modulation schemes have demonstrated inefficient performance when channel coefficients fluctuate randomly. By altering modulation schemes adaptively for transmission in a CR system, in fading channel conditions, a higher throughput while maintaining an acceptable BER rate can be achieved. Further, the thesis looks at the basic concepts of CR, the problems of fixed spectrum allocation methods and how CR can overcome the spectrum scarcity problems. The project also investigates how signal fading affect the received power and how adaptive modulation can be employed to maintain the required bit error rate. In addition, a range of techniques to monitor SNR was investigated and suitable SNR estimators were developed to be able to cope with both slow Rayleigh fading and very fast Rayleigh fading to eventually see how adaptive modulation helps in improving performance at a given BER constraint.

1.1 Cognitive Radio

According to the encyclopedia of Computer Science, there is a three-point computational view of cognition as follows:

1. Mental States and Processes intervene between input stimuli and output responses
2. The mental states and processes are described by algorithms
3. The mental states and processes lend themselves to scientific investigations

From Pfeifer and Scheier [6] we gather that the interdisciplinary study of cognition is concerned with exploring general principles of intelligence through a synthetic methodology termed learning by understanding. In light of these definitions, and bearing in mind that cognitive radio is aimed at improved utilisation of the radio spectrum, Simon Haykin [7] defined cognitive radio as an intelligent wireless communication system that is aware of its surrounding environment (that is outside world), and uses the methodology of understanding-by-building to learn from the environment and adapt its internal states to statistical variations in the incoming Radio Frequency stimuli by making corresponding changes in certain operating parameters (example, transmit-power, carrier-frequency, and modulation strategy) in real-time, with two primary objectives in mind which are:

- Highly reliable communications whenever and wherever needed
- efficient utilisation of the radio spectrum

The important keywords standing from this definition are awareness, intelligence, learning, adaptivity, reliability and efficiency. Fortunately, implementation of this set

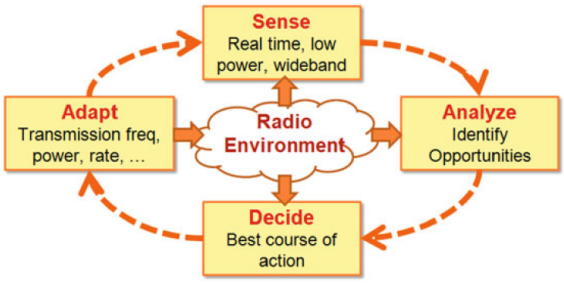

Figure 1.1: Functional Architecture of a Cognitive Radio

of capabilities is now feasible, owing to the advances in digital signal processing, networking, machine learning, computer software and computer hardware. In the same breath, the IEEE 1900.1 group tasked to define cognitive radio came up with the following definition: " A type of radio that can sense and autonomously reason about its environment and adapt accordingly. This radio could employ knowledge representation, automated reasoning, and machine learning mechanisms in establishing, conducting, or terminating communication or networking functions with other radios as shown in Fig 1.1. Cognitive radios can be trained to dynamically and autonomously adjust its operating parameters".

In summary, CR are wireless systems, in which communication does not take place in a fixed or an assigned band of frequency. The radios continuously sense the immediate Radio Frequency environment and operate in a band that is available and suitable, dynamically adjusting their modulation, frequency, coding, power and other parameters to make the most efficient use of the vacant spectrum while keeping interference to existing systems to a minimum.

The above definitions of CR assume that cognition will be implemented as a control process, as part of a software defined radio, hence implying autonomous operation. Important features of CR are:

- Observation: the radio can sense and acquire information about its operating RF environment, directly or indirectly
- Adaptability: the radio can adapt to various electromagnetic environments and various channel conditions
- Intelligence: the radio learns and can apply the information towards a specific goal, such as improving performance

1.2 Operation of a cognitive radio

Cognitive radio networks (CRN) require a radio device that is very flexible, to enable it to change radically various protocol functions at runtime. Software-defined radios(SDR) are an ideal platform for CRNs. Most radios today implement almost all physical layer

processing and some MAC protocol functions in hardware, limiting the degree of runtime adaptivity to a small predefined set of changes, for example, choosing between a handful of transmission rates. On the other hand, SDRs, attempt to do as much processing as possible in the digital domain.

1.2.1 Stages of cognitive radio operation

The cognitive process starts with the passive sensing of Radio Frequency stimuli and culminates with action. The three main online cognitive tasks are [7]

- Radio-scene analysis, which encompasses the following: 1) Estimation of interference temperature of the radio environment and 2) detection of spectrum holes
- Channel Identification, which encompasses the following: 1) estimation of the channel-state information (CSI) and 2) prediction of channel capacity for use by the transmitter
- Transmit-power control and dynamic spectrum management

The first two stages of a cognitive radio operation take place on the receiver side and the last stage takes place on the transmitter side [7]

1.2.2 Cognition Cycle

Through interaction with the radio frequency environment, these three tasks above form a cognitive cycle, which is shown in the picture below in 1.2. It is evident that the the cognitive module in the transmitter must work in a harmonious way with the cognitive components in the receiver and in order to keep this harmony between the cognitive radio's transmitter and receiver at all times, a feedback channel linking the receiver to the transmitter need to be established. The receiver can then send information on the performance of the forward link to the transmitter, demonstrating the fact that the CR is an example of a feedback communication system.

A broadly defined CR technology accomodates a scale of differing degrees of cognition. At one end of the scale, the user may select a spectrum hole and build its cognitive cycle around that hole. On the other end of the scale, the user may make use of multiple implementation technologies to build its cognitive cycle around a wideband spectrum hole or set of narrowband spectrum holes to give the best expected performance in terms of spectrum management and transmit-power control, in the most secure way possible.

1.2.3 Physical Architecture of a Cognitive Radio

The main components of a CR transceiver are the baseband processing unit and the radio front-end. To be able to adapt to the time-varying radio frequency environment, the components can be reconfigured via a control bus. When the signal is received at

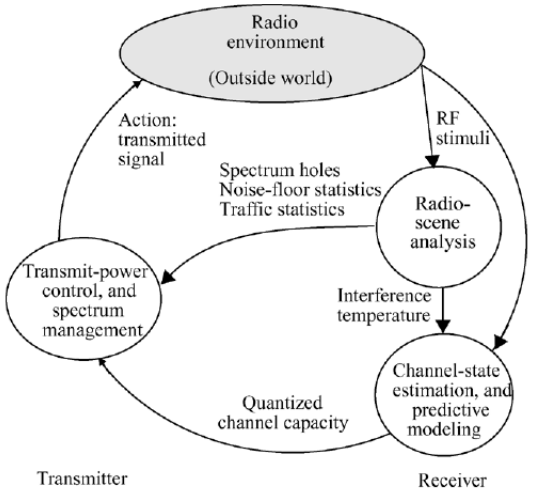

Figure 1.2: Basic cognitive cycle

the RF front end, it is amplied, mixed and passed through to an Analog to Digital converter. The signal is then modulated/demodulated and encoded or decoded. Though the baseband processing unit of a CR is similar to existing tranceivers, the new feature of a CR transceiver is the wideband sensing capability of its RF front-end. This function is primarily related to the radio frequency hardware technologies such as wideband antenna, adaptive filters and power amplifiers. As a matter of fact, cognitive radio radio frequency hardware should be able to detect and work in any segment of a large range of the spectrum. Figure 1.3 depicts the a general architecture fo a cognitive radio and it has the following components as shown [8]

1. Low Noise Amplifier: The LNA reduces the noise component and amplifies the desired signal

2. RF filter: The RF filter selects the appropriate band, using a band pass filter at the receiver

3. Mixer: The mixer multiplies the received signal with a locally generated RF signal and converts it to the baseband or the intermediate frequency (IF) signal.

4. Voltage Controlled Oscillator (VCO): The VCO generates a sinusoid to multiply the received signal and convert it to either an IF or baseband signal

5. Phase locked loop (PLL): The main task of a PLL is to make sure the signal is locked at a specific frequency and to generate accurate and precise frequencies with fine resolution

6. Channel Selection Filter: The channel selection filter is used to choose the desired channel and reject unwanted channels

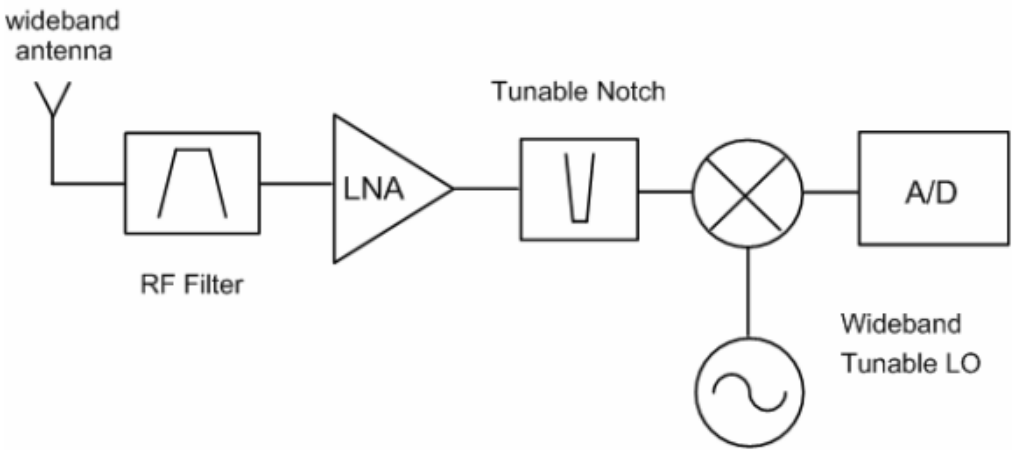

Figure 1.3: Physical Architecture of a Cognitive Radio

7. Tunable Notch Filter: Tunable notch filter is an essential component to suppress the out-of-band interference signals due to the large number of potential transmitters in the wide operating frequency range

8. Automatic Gain Control (AGC): The AGC's purpose is to keep and maintain a stable constant output power level of an amplifier over a wide range of input signal levels

The requirement that cognitive radio communication is strictly conditional on the reliable detection of unoccupied spectrum establishes a new type of functionality on the physical layer for spectrum sensing over all available degrees of freedom, be it time, frequency and space, to be able to identify frequency bands currently available for transmission. The main challenge of spectrum sensing is the detection of weak signals in noise with very small probability of miss detection. Spectrum sensing requires the radio to receive a wide band signal through an RF front-end sample it by high speed analogue to digital converter (A/D) and perform measurements for detection of primary user signals, as illustrated in Figure 1.5. The challenges in spectrum sensing are : 1) achieving sufficient RF front-end sensitivity for wideband signals; and secondly 2) accurately detecting non-similar, frequency band dependent, primary signals at differing received power levels. Having then identified an available spectrum segment, a cognitive radio should employ modulation schemes that provide the best spectrum utilisation and capacity while avoiding interference to any primary user. In addition, the preferred transmission scheme should be flexible enough to allow assignments of any band to any user, and should be scalable with the number of users and bands. In the best case scenario, this flexible wideband transmission would be made possible by digital waveform synthesis, where a set of parameters specifies transmission bands and power control. Figure 1.4 illustrates the top-level architecture of a wideband transmitter. As mentioned, the primary challenge is to create a signal that adaptively changes the occupied bandwidth and without causing

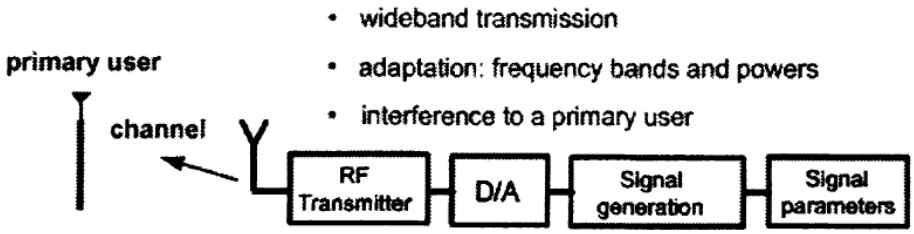

(b) Cognitive radio transmitter

Figure 1.4: CR transmitter

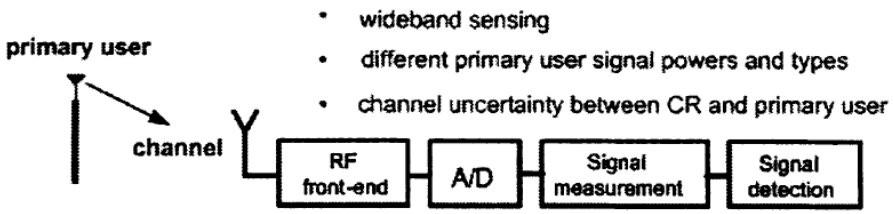

Figure 1.5: CR receiver

interference to any active primary users, without any external analogue filters.

Going back to Fig 1.3 architecture of a wideband RF front-end capable of simultaneously sensing several Ghz wide spectrum, this architecture is usually proposed for software-defined radios [7]. The wideband RF signal presented at the antenna of such a front-end includes signals from close and widely spaced transmitters , and from transmitters operating at widely different power and channel bandwidths. Hence, the RF front-end should be able to detect a weak signal in a large dynamic range, though this capability requires a high speed analogue to digital converter with high resolution which may not be feasible in practice.The requirement of a high speed A/D converter requires the dynamic range of the signal to be reduced before A/D conversion and this can be achieved by filtering the strong signals. As strong signals can be located anywhere in the wide spectrum range, a notch filter can be used. Alternatively, dynamic range reduction can be achieved by filtering the signal in the spatial domain, instead of the frequency domain using multiple antennas, inspired from [9] that found out that spatially received signals occupy a limited number of directions or spatial clusters. Therefore, antenna arrays through beamforming techniques can be used to selectively receive or suppress signals. Conclusively, as far as the physical architecture of the Cognitive radio is concerned, the key challenge is the accurate detection of weak signals of licensed users over a wide spectrum range, proving that special focus should be given to the implementation of the RF-wideband front end and A/D converter.

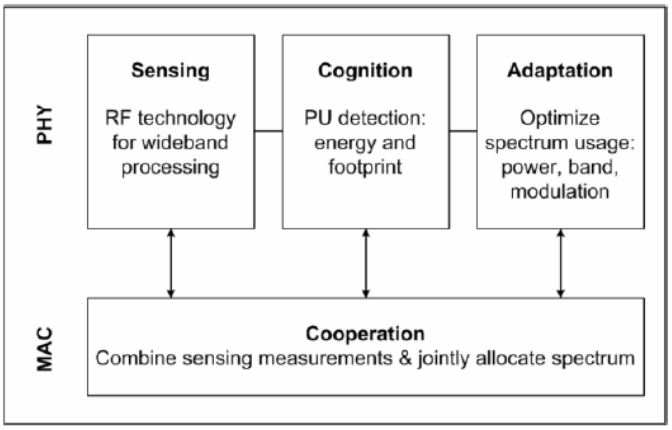

Figure 1.6: Cross layer functionalities

1.3 Spectrum Sensing

As previously mentioned a Cognitive Radio is a radio that is able to sense the spectral environment over a wide frequency band and use this information to its advantage to opportunistically provide wireless links that best meet the user communication requirements. Even though there are many other characteristics,for simplicity, a more restricted definition and the physical (PHY) and medium access control (MAC) functions that are linked to spectrum sensing as shown in Fig 1.6 is considered. Since Cognitive Radios are considered lower priority or secondary users of spectrum allocated to a primary user, a fundamental requirement is to minimise interference to potential primary users in their surrounding. On the other hand, primary user networks do not have any requirement to change their infrastructure for spectrum sharing with cognitive networks. As a result Cognitive Radios should be able to detect primary user presence independently through continuous spectrum sensing.

1.4 Scope

In this section, we outline the aims and what areas were tackled throughout the chapters in this thesis. We will consider a Spectrum Sharing Cognitive Radio Network model with one Primary Network (PN) and Secondary Network (SN). The primary user (PU) and secondary (SU) share the same channel band for data transmission and all links are assumed as fading channels with AWGN. Moreover, the secondary link employs adaptive modulation in conjunction with power control and assumes the SU receiver obtains accurate estimate of the channel state information.

1.4.1 Aims

In more depth, we aim to investigate how varying the modulation scheme in a Cognitive Radio (CR) time-varying environment can impact the performance positively. The channel of a wireless communication system is characterised by Doppler Spread, multipath fading, scattering, shadowing which results in random fluctuations in radio channels. The primary objective of this project is to develop analytical methods and tools as well as devise computer simulations to investigate how adaptive modulation technique can exploit the rapid fluctuations in wireless channels to maximise Bandwidth usage, optimise power usage and eventually operate in spectral efficient ways, while maintaining the required BER constraint and data rate. Considerable work has been done, assuming slow fading Rayleigh system. This thesis also aims, in a first instance to analyse performance by looking at slow fading systems but also investigate how very fast fading affects Cognitive Radio's BER performance and finally how Adaptive modulation Technique can contribute to improving performance. Though we will not go deep in channel delay and co-channel interference, this thesis will also take note how these factors affect performance in a cognitive radio system.

1.4.2 Thesis Overview

The first chapter overviews the CR process, emphasizes the importance of spectrum sensing and sets out the aims and objectives of this thesis, including the main assumptions to be considered. Next, the second chapter, considers adaptive modulation from a theoretical standpoint, giving expressions for probability of error in AWGN and multipath fading environments. An attempt at implementing a blind SNR monitoring technique is made and new developments were made in this respect to render it fully functional in an adaptive system employing MPSK modulation scheme. Chapter 3 outlines the system model used, and lay the groundwork by considering adaptive modulation in a SSCRN system by featuring analytical methods and results showing the effectiveness of adaptive techniques. Chapter 4 describes the simulation program and the procedures used. Chapter 5, describes the results and finally Chapter 6 concludes this thesis.

Chapter 2

Adaptive Modulation Techniques

The channel of a wireless communication system is characterised by frequency, time dispersion, multipath fading, as the previous chapter expounded, result in random fluctuations in radio channels. More precisely mobile radio links can exhibit severe multipath fading which leads to serious degradation in the signal-to-noise ratio (SNR) and consequently a higher bit error rate (BER). Techniques such as increased link budget margin or interleaving with channel coding are usual fading compensation mechanisms required to improve link performance. These techniques are, however, designed relative to the worst-case channel conditions, resulting in poor utilisation of the full channel capacity a fair amount of the time, that is under shallow or negligible fading). Adapting certain parameters of the transmitted signal to the channel fading leads to a better utilisation of the channel capacity [10]. The basic concept behind adaptive transmission is real-time balancing of the link budget through adaptive variation of the transmitted power level, symbol transmission rate, constellation size, coding rate/scheme or any combination of these parameters [11], [12], [13], [14], [15]. These schemes provide a higher average link spectral efficiency by exploiting the time-varying nature of wireless channels, without taking a toll on BER or wasting power: transmitting at high speeds under favourable channel conditions and responding to channel degradation through a smooth reduction of their data throughput. Understandably, to achieve a good performance from these schemes, accurate channel estimation at the receiver and a reliable feedback path between that estimator and the transmitter is required. Moreover, the outage probability of such schemes, discussed later in this section can be quite high, mainly for channels with low average SNR, and hence requiring buffering of input data. Adaptive systems are best suited for applications without strict delay constraints.

2.1 Adaptive Modulation Model for Cognitive Radio

In the real world, channel condition fluctuate dynamically, and since fixed modulation schemes are built, based on worst case scenario to give an acceptable bit error rate performance, these systems do not perform well as they cannot take advantage of the different channel conditions. Adaptive modulation is a technique that can adapt the transmission

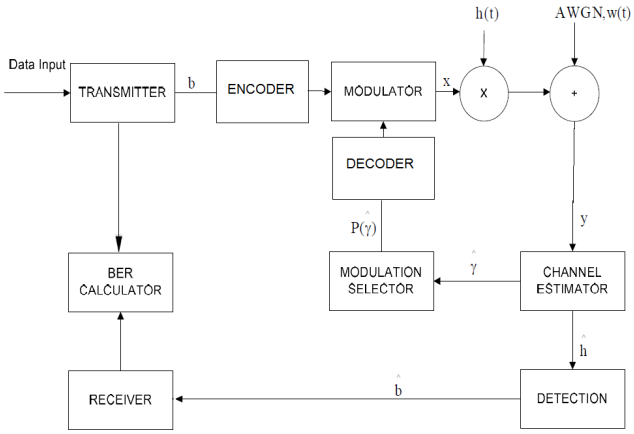

Figure 2.1: Basic model of a cognitive radio with adaptive modulation capability

scheme to the current channel characteristics, and by exploiting the time-varying nature of the wireless channels, adaptive modulation based systems change transmission parameters like power, data rate, coding and modulation schemes, or any combination of these in accordance with the state of the channel [16]. With this technique, a more robust and spectrally efficient communication system over multi-path fading channels is put in place. If the channel can be estimated properly, the transmitter can adapt to the current channel conditions easily by altering the modulation schemes while meeting the required BER. This can be done by estimating the channel at the receiver and through a feedback channel relay this estimate back to the transmitter. Figure 2.1 illustrates a basic block diagram of an adaptive modulation based cognitive radio system. Note that there is also an encoder and decoder component in the block diagram can complement an adaptive modulation system for a more resilient and better performance. Looking at the block diagram, it can be seen that a data stream, b(t), is first encoded, then modulated using a modulation scheme given by $P_k(\gamma)$, which is the probability of selecting k^{th} modulation mode from K possible modulation schemes available at the transmitter, which is a function of the estimated SNR of the channel.

The signal reaching the receiver can be modelled as:

$$y(t) = h(t)x(t) + w(t) \tag{2.1}$$

From equation (2.1), y(t) is the received signal, h(t) is the fading channel impulse response, and w(t) is the additive white Gaussian noise (AWGN). The estimated channel information is relayed back to the transmitter that makes decision on next modulation scheme to be applied on each packet of data. The channel state information, $\hat{h}(t)$, also gets sent to the demodulator or detection component of the receiver to help in demodulating the data stream. Finally the data is decoded at the receiver. In [16],the adaptive communication system is described as follows: A pilot tone continually sends a known "channel sounding" sequence so that the channel-induced envelope fluctuation, α and phase shift,

ϕ can be extracted at the channel estimation stage.Using the channel gain estimate $\hat{\alpha}$, a decision device selects the rate and power to be transmitted configures the demodulator accordingly and relays this decision to the transmitter via the feedback path.

2.1.1 ACM Protocol and Assumptions

For a good performance, the modulator and demodulator must be configured at any instant for the same constellation size or modulation scheme. This warrants the need for an error-free feedback path, though in reality such schemes inevitably introduce a certain time delay, $\tau_{f_b}[s]$, which may include decoding/ARQ delay, and propagation time via the feedback path. So, even if the channel conditions are estimated perfectly and relayed to the receiver, the system will not be able to adapt to the channel fading but rather to at best a τ_{f_b} delayed version of it. Choosing power or the constellation size is based on the channel estimate at time t, but the data are sent over the channel at time $t+\tau$ such that $\tau_{f_b} \leq \tau \leq \tau_t$, where $1/\tau_t$ is the rate at which we change the constellation size and power. The aim is to operate with the smallest possible τ_{f_b} to minimise the impact of the feedback delay, and with the largest possible τ_t to minimise the rate of system reconfiguration [16]. We assume no channel delay and perfect channel statistics across the feedback path, to reduce implementation complexity in this thesis.

2.1.2 Modulation Schemes and BER analysis

Digital modulation is a method of encoding information for transmission. Information to be transmitted is turned into a series of digital bits, the 0s and 1s of computer binary language. At the receiving end, the information is then decoded and processed. In the last few years, there has been a major shift from the simple amplitude modulation (AM) and frequency modulation (FM) to digital techniques such as Quadrature Phase Shift Keying (QPSK), Frequency Shift Keying (FSK), Minimum Shift Keying (MSK) and Quadrature Amplitude Modulation (QAM). Digital terrestrial microwave designers focus on bandwidth efficiency and lower error rate while power efficiency is not primordial since they have plenty available. However, the situation is very different for handheld cellular phone designers, who need to focus on power efficiency because all handheld cellular phones are battery running devices. In that sense, power efficiency is of utmost importance. Focusing on improving one parameter (power, cost or bandwidth) will require sacrificing other parameters. The variation of the property of a signal, such as its amplitude, frequency or phase is called modulation and the different types of modulation techniques available are Amplitude Shift Keying (ASK), Frequency Shift Keying (FSK), and Phase Shift Keying (PSK) [17]. There are different types of modulation that are used in Adaptive Modulation, such as Phase Shift Keying (PSK) that consists from the use of a carrier's phase with the transmitted bit stream for some particular cases from phase shift keying (PSK) with various number from values M, to representation various cases from PSK, like, binary phase shift keying (BPSK), quadrature phase shift keying (QPSK), 8-PSK, 16-PSK, 64-PSK, and so on where $M = 2^i$ and $i = 1$,2,3,4 to n.

We first consider BPSK modulation with coherent detection and perfect recovery of the carrier frequency and phase. With binary modulation each symbol corresponds to one bit, so the symbol and the bit error rates are the same. The transmitted signal is $s_1(t) = Ag(t)\cos(2\pi f_c t)$ to send a 0 bit and $s_2(t) = Ag(t)\cos(2\pi f_c t)$ to send a 1 bit, where A is the amplitude of the signal, $g(t)$ is the baseband pulse-shaping filter to improve the spectral characteristics of the transmitted signal. From chapter 5 in [18], we have the probability of bit error, P_b ,is

$$P_b = Q(\frac{d_{min}}{\sqrt{2N_o}}) \tag{2.2}$$

Where:

$$Q(x) = \int_x^\infty \frac{1}{\sqrt{2\pi}} \exp(-\frac{z^2}{2})dz \tag{2.3}$$

And, d_{min} is the minimum distance between signal constellations, N_0 is the noise spectral density. From Chapter 5 in [18] for $M = 2$, where M is the modulation order or the number of symbols on the constellation, we have $d_{min} = \|s_1 - s_0\| = \|A - (-A)\| = 2A$. Relating A to the energy-per-bit, E_b, we have

$$E_b = \int_0^{T_b} s_1^2(t)dt = \int_0^{T_b} s_1^2(t)dt = \int_0^{T_b} A^2 g^2(t)\cos^2(2\pi f_c t)dt = A^2 \tag{2.4}$$

Where f_c is the centre frequency and T_b is the time to transmit 1 bit. Thus, the signal constellation for BPSK in terms of energy-per-bit is given by $s_0 = \sqrt{(E_b)}$ and $s_1 = -\sqrt{(E_b)}$. This yields the minimum distance $d_{min} = 2A = 2\sqrt{(E_b)}$. Substituting this into equation (2.5) yields

$$P_b = Q(\frac{2\sqrt{E_b}}{\sqrt{2N_o}}) = Q(\sqrt{\frac{2E_b}{N_o}}) \tag{2.5}$$

QPSK modulation, $M = 4$, consists of BPSK modulation on both the in-phase and quadrature components of the signal. With perfect phase and carrier recovery, the received signal components corresponding to each of these branches are orthogonal. Therefore, the bit error probability on each branch is the same as for BPSK. Hence the probability bit error in QPSK corresponds to the equation (2.5). As QPSK yields the same BER as BPSK, though the QPSK bit rate is twice the BPSK bit rate, the BPSK modulation scheme is inefficient in bandwidth usage. The symbol error probability formula, for AWGN channel conditions can be extended as follows (2.6):

$$P_b \approx \frac{2}{\log_2 M} Q\left(\sqrt{\frac{2E_b Log_2 M}{N_0}} \sin\left(\frac{\pi}{M}\right)\right) \tag{2.6}$$

PSK is not utilised for higher order, M greater than 8, because of the BER being much higher than the QPSK BER. MQAM is used in many applications and is a practical modulation scheme technique that can achieve better BER than MPSK. The BER for MQAM over the AWGN channel is given by 2.7.

$$P_b = \frac{4}{\log_2 M}\left(1 - \frac{1}{\sqrt{M}}\right) Q\left(\sqrt{\frac{2E_b Log_2 M}{(M-1)N_0}}\right) \tag{2.7}$$

Adaptive modulation technique's aim is to use various order modulations, switching to higher order, and sending more bits/symbol resulting in higher spectral efficiency and data throughput when the channel conditions is favourable and switching to a lower order and more robust modulation to withstand signal fading and interference and maintain the required BER.

2.1.3 Rayleigh Fading Channel

Rayleigh fading is a statistical model that characterises the effects of a propagation environment on a radio signal. This model assumes that the received signal, varies randomly or fade according to a Rayleigh distribution. Rayleigh fading can be used as a reasonable model for tropospheric and ionospheric signal propagation as well as urban and indoor multipath propagation [10]. It is commonly used to model situations where there is less or no dominant propagation along a line of sight between the transmitter and receiver. Throughout this thesis, we consider the Rayleigh fading channel, as the channel model between PU's and SU's. The Rayleigh PDF basically is the square root of the sum of two independent and identically distributed zero mean Gaussian random variable. In other words, If R_1 and R_2 are independent and identically distributed zero mean Gaussian variables, the Rayleigh variables, R will be:

$$R = \sqrt{R_1^2 + R_2^2} \tag{2.8}$$

And the PDF is:

$$p_r(r) = \frac{r}{\alpha^2} \exp\left(-\frac{r^2}{2\alpha}\right), \ \alpha \geq 0 \tag{2.9}$$

Where r is the envelope amplitude of the received signal and $2\alpha^2$ is the pre-detection mean of the multipath signal.

2.1.4 Switching Levels

In [19], the received signal Signal to Noise Ratio (SNR) , s, is compared with N switching levels, l_n, and an appropriate modulation scheme is selected accordingly. From the work of Kamio et al [20], the modulation scheme that is used is selected as follows: [to reduce implementation complexity of the modulator and demodulator in this thesis, we will consider only M-ARY PSK systems], hence:

$$Modulation\ Scheme = \begin{cases} No\ Transmission\ if\ l_1 > s \\ QPSK\ if\ l_1 \leq s < l_2 \\ 8PSK\ if\ l_2 \leq s < l_3 \\ 16PSK\ if\ s \geq l_4 \end{cases}$$

where l_n are values from the quasi-static AWGN channel and s, as previouly stated is the received signal, SNR.

2.2 SNR monitoring techniques

Signal-to-noise ratio(SNR) measurement is commonly used in digital communications as many techniques and components need SNR information in their implementation. From power control in [21]to applications such as maximal ratio combining and recently importance of knowing the instantaneous SNR has gained more momentum, with the use of adaptive techniques, mobile assisted hand-off, dynamic spectrum access, cognitive radio and feedback-assisted resource allocation [22]. The presence of the idea of cognitive radios introduces some new techniques like spectrum sensing and sharing and some of these methods require SNR as an essential parameter to function.

In addition, the nature of cognitive radios make them work under low SNR, mainly in spectrum sharing scenarios, where a limit on cognitive user transmit power is imposed to control interference on primary users. In [23], a maximum-likelihood SNR estimator for cognitive radio was proposed, which is used to control the transmitted power in a detect and avoid cognitive technique. Added to this, there has been a number of studies done on the effect of SNR on cognitive systems, with different models and different realisations of the communication channel [24] [25] [23] [26]

2.2.1 SNR Estimators Categories

SNR estimation techniques can be classified as Data-Aided (DA), Decision-Directed (DD), and Non Data-Aided (NDA) estimators. DA estimators like the one in [26] make use of transmitted pilot symbols to compute their estimates. A DA estimator for Single Input Multi Output (SIMO) systems has been presented in [27]. In fact, having pilot systems take a toll in the system throughput, which is the primary disadvantage of this type

of estimators. Moreover, in cognitive radio systems, DA cannot be applied in cognitive radio systems, where the primary users's pilot symbol locations might not be known to the secondary users. On the other hand, DD estimators can be considered as a special case of DA estimators when the pilot symbols are replaced with the output of the decoder [28]. NDA estimators do not need to know about the transmitted signal, hence allowing in-service and inter-systems SNR estimation.

SNR estimators can be classified in a different way; namely, I/Q based and envelope-based (EVB) estimators. I/Q based estimators need coherent detection as they require in-phase and quadrature components of the signal. I/Q estimators use the Expectation Maximisation (EM) algorithm to get the Maximum Likelihood estimate [29] [27]. It is worthwhile noting that the performance of I/Q-based estimators is heavily impacted by I/Q degradation. However, EVB estimators can be used with an I/Q imbalanced signal as they only use the signal magnitude as parameters. Given, EVB estimators are more resilient to I/Q imbalance, this is clearly a good advantage for cases where SNR estimation is required before synchronisation or equalisation.

2.2.2 Moments based EVB estimator

In [30] [31] [32], SNR estimation for signals transmitted though Nakagami fading channels have been considered. The moments-based EVB estimator in Nakagami-m fading channels described in [32] has been proven to fail under constant amplitude constellations, for example M-ary PSK signals), as it was analytically proven that the value of the fourth moment, of the constant amplitude constellations is equal to the square of the value of the second moment, rendering the ratio between the two moments a constant value, completely independent of the SNR. In addition, the SNR estimator in [31] required interpolation and lookup tables to compute the SNR estimate, which inferred a higher mathematical complexity and required more storage. Moreover, it was dependent on the modulation scheme or received signal constellation, that required apriori knowledge of the received signal constellation and also warranted the need for an increase in the storage resources for lookup tables with the increase in the number of supported constellations, mainly for adaptive modulation systems.

2.2.3 Blind moments based EVB SNR estimator

In his newly published paper, Hafez et al [22] presents a similar moments based EVB estimator but in a new context of SNR estimation for time-domain Gaussian-distributed signal. Among the features of this new SNR estimator, it utilises the received domain signal to get an estimate of the SNR, therefore not requiring synchronisation. In addition, when used for Gaussian-distributed signals for example, OFDM signals, the operation and performance of the moments-based estimator are shown to be independent of the received signal constellation, thereby allowing its operation under all types of signal constellations, which include constant amplitude constellations for example, M-ary PSK, in contrast to the results presented in [32]. Hafez et al [22] derived and proved analytically in [22] and

also it is a low complexity implementation in comparison to the one presented in [32].

We consider a digital communication system over a time varying channel, where the coherence time of the channel, $\tau_c = 1/f_d$, where f_d is the Doppler spread, is smaller than the transmitter symbol duration. Moreover, assuming the channel delay spread, τ_d, is lot smaller than the symbol duration, which means that inter-symbol-interference, ISI is ignored, hence the received signal, r_n is given by

$$r_n = g_n s_n + w_n \tag{2.10}$$

Where N is the number of samples in a symbol, referred to as the symbol size, g_n is the fading channel gain, s_n is the transmitted signal samples and w_n is a complex zero-mean white Gaussian noise with variance equal to $2\sigma_w^2$. The channel gain, g_n is modeled as a zero-mean complex random variable and can be written as $g_n = g_n e^{j\phi}$ with ϕ taking values between $-\pi$ and π under any arbitrary distribution. The phase distribution is not of concern to the EVB estimator which is not dependent on the phase of the signal. $|g_n|$ follows the Nakagami-m distribution:

$$f_{|g_n|}(|g_n|) = \frac{2}{\Gamma(m)} \left(\frac{m}{\alpha_g^2}\right)^m |g_n|^{2m-1} \exp\left(-\frac{m|g_n|^2}{\alpha_g^2}\right) \tag{2.11}$$

where $\alpha_g^2 = E(|g_n|^2)$ and Γ is the gamma function. Moreover, it should be pointed out that $|g_n|$ and ϕ are independent. The Nakagami-m distribution approximates a Rician distribution for the fading parameter m in the range $1 < m < \infty$ and approximates a Hoyt or Nakagami-q distribution for m in the range $0.5 \leq m < 1$, while it becomes a Rayleigh distribution for $m = 1$.

In general, moment based estimators are suitable for Gaussian distributed signals, described as follows:

$$s_n = I_n + jQ_n \tag{2.12}$$

where s_n is a signal where the real I_n and imaginary Q_n parts of the complex time domain signal are both Gaussian random variables. The signal envelope $|s_n|$ follows the Rayleigh distribution,

$$f_{|s_n|}(|s_n|) = \frac{|s_n|}{\sigma^2} e^{-\frac{|s_n|^2}{2\sigma^2}} \tag{2.13}$$

where $\sigma^2 = Var(I_k) = Var(Q_k) = 1/2$, for a unit power transmitted signal. Hence, the SNR can be formulated as:

$$\rho = \frac{\alpha_g^2}{2\sigma_w^2} \tag{2.14}$$

Proposed Estimator

We want to compute the estimate of the SNR using the ratio of the different moments of the received-time domain signal, which is commonly known as the method of moments [33]. The probability density function of r_n, conditioned on both g_n and s_n , given by:

$$p(|r_n||g_n, s_n) = \frac{|r_n|}{\sigma_w^2}\exp\left(-\frac{|g_n|^2|s_n|^2 + |r_n|^2}{2\sigma_w^2}\right) \times I_0\left(\frac{|r_n||g_n||s_n|}{\sigma_w^2}\right) \tag{2.15}$$

where $I_0(.)$ is the modified Bessel fnction of the first kind and order zero leading to:

$$E[|r_n|^l] = \int_0^\infty 2^{l/2}\Gamma\left(\frac{l}{2}+1\right)\sigma_w^l e^{-|s_n|^2}\left(\frac{m}{m+\rho|s_n|^2}\right)^m \times {}_2F_1\left(\frac{l}{2}+1, m, 1; \frac{\rho|s_n|^2}{m+\rho|s_n|^2}\right) d|s_n|^2, | \tag{2.16}$$

where ${}_2F_1(a, b, c; x)$ is the Gauss Hypergeometric function [34]. Using the ratio between the fourth and second moments of the time domain signal to get the estimate of the SNR. Defining z as the estimation parameter, we obtain:

$$z = \frac{M_4}{M_2^2} = f(\rho) \tag{2.17}$$

$$M_l = E[|r_n|^l],\ l \in 2, 4 \tag{2.18}$$

$$\rho = f^{-1}(z) \tag{2.19}$$

As M_l is not available in practice, the following estimate is based on the symbols of the received signal

$$\hat{M}_l = \frac{1}{P}\sum_{p=1}^{P}|r_p|^l,\ l \in 2, 4 \tag{2.20}$$

where $\hat{M}_l$ is the average of the square of the absolute value of the received symbols, raised to the l^{th} power and P is the number of data symbols used to get the estimate of the moments:

$$\hat{z} = \frac{\hat{M}_4}{\hat{M}_2^2} \tag{2.21}$$

$$\text{and } \hat{\rho} = f^{-1}(\hat{z}) \tag{2.22}$$

The inverse function can be implemented using lookup tables or polynomial approximation or using the direct formula. This estimator being independent of the signal constellation gives it the advantage of being suitable for adaptive systems as only one

ESTIMATOR BLOCK IMPLEMENTATION ALGORITHM

initiate P

$i = 0$
$\hat{M}_2 = 0$
$\hat{M}_4 = 0$
while $i < P$
$x = abs(r_i)^2$
$y = x^2$
$\hat{M}_2 = \hat{M}_2 + x$
$\hat{M}_4 = \hat{M}_4 + y$
$i = i + 1$
end
$\hat{z} = \frac{\hat{M}_4}{\hat{M}_2^2}$
$\hat{\rho} = f^{-1}(\hat{z})$ *achived by plugging* $\hat{z}$ *in place of* z *in* 2.33

Figure 2.2: Estimator Algorithm

inverse function is needed for all different constellations. The second and fourth moments were chosen as higher order moments will lead to a more complex relation between ρ and z, which can be non-invertible. Figure 2.2 below demonstrates that the estimator is relatively easy and simple to implement, requires minimal memory resources and its complexity is directly proportional to the number of data symbols used in estimation, that is the estimator is of order P.

Based on theorem 1, proved in appendix, [22], we can rewrite equations (2.18) and (2.19) as:

$$z = 2\frac{(1 + 2\rho + \gamma_m\rho^2)}{1 + 2\rho + \rho^2} \tag{2.23}$$

and

$$\rho = \frac{z - 2}{2\gamma_m - z} + \frac{\sqrt{2}\sqrt{(z-2)(\gamma_m - 1)}}{2\gamma_m - z}, \; 2 < z < 2\gamma_m \tag{2.24}$$

where $2\gamma_m$ is the upper limit of the estimation parameter, which is related to the Nakagami-m parameter through the following relation

$$\gamma_m = \frac{m + 1}{m} \tag{2.25}$$

We assume the value of m is known, which can be estimated using one of the methods presented in [35]. Theorem 1 from Hafez et al [22] proved that the estimator is totally independent of the signal constellation and it can be easily shown that equation (2.23) is also valid for the case where the system is affected by a Gaussian interference. Hence $\rho = \sigma^2/2(\sigma_w^2 + \sigma_I^2)$, where ρ represents the Signal to Interference plus Noise Ratio(SINR) and σ_I^2 is the power of Gaussian interference.

2.3 Conclusion

We choose the moments-based EVB estimator proposed by Hafez et al [22], due to the fact that is a blind estimator that is simple to implement and unlike [32], it does not fail under constant amplitude constellations and operates under all types of signal constellations, including M-ary PSK, which is will be considered throughout this thesis. Before delving deeper and start designing the adaptive modulation system for the CR, we now develop analytical methods to gauge the effectiveness of implementing adaptive modulation in a spectrum sharing cognitive radio network in the next chapter.

Chapter 3

Performance of Adaptive Modulation In Cognitive Radio Networks

In this chapter, we will outline the model underpinning the performance study of Adaptive modulation techniques employed in Cognitive Radio Network. We consider an OSA CRN model, which allows the SUs to opportunistically utilize the licensed spectrum only when the PU is inactive. Given that the SU is effectively utilizing the available channels, when PU is not transmitting interference issues can be ignored. The system model is illustrated in Fig. 3.1, showing the components of the secondary network, including the transmitter, SU-TX, and the receiver, SU-RX. There is an ideal power control mechanism in place that determines the instantaneous transmit power, $P_{\mathrm{t,16PSK}}$, to maintain the BER when 16PSK modulation is employed. To maximize spectral efficiency, the system implements adaptive modulation, and it does so by switching to the more robust QPSK modulation in the event of channel fades, and the instantaneous transmit power $P_{\mathrm{t,QPSK}}$ is determined accordingly. To this end, the feedback channel has to relay a sufficiently accurate Signal-to-Noise Ratio (SNR), γ, with minimal delay. We assume that the transmitter obtains the SNR estimate instantly; that is, there is no feedback channel delay. In addition, we also assume coherent reception with perfect carrier phase estimation throughout this work. Next, looking at channel selection, we have a set of N channels and the probability that any particular channel is available is P_{a}. With the help of spectrum sensing information, the SU-TX selects the appropriate channels. Work carried out in [36] treats power control in OSA CRN in depth, although in this thesis we assume that spectrum sensing is ideal hence ignoring the implications of misdetection. In the case where the SU is employing 16PSK modulation, we need one channel for transmission and there is a channel outage if all the N channels are taken. If the transmit power, $P_{\mathrm{t,16PSK}}$, exceeds the regulatory peak power, $P_{\max}$, the system switches to QPSK modulation to maintain the BER requirement. Channel outage occurs if that transmit power, $P_{\mathrm{t,QPSK}}$, exceeds $P_{\max}$ or if there is no pair of adjacent channels available for transmission. Note that, to employ QPSK modulation, the SU transmitter will need twice as much bandwidth as with 16PSK modulation, because the data rate is maintained. Therefore the QPSK modulation requires two adjacent channels for transmission. Finally, we assume that the channels are slowly varying Rayleigh flat

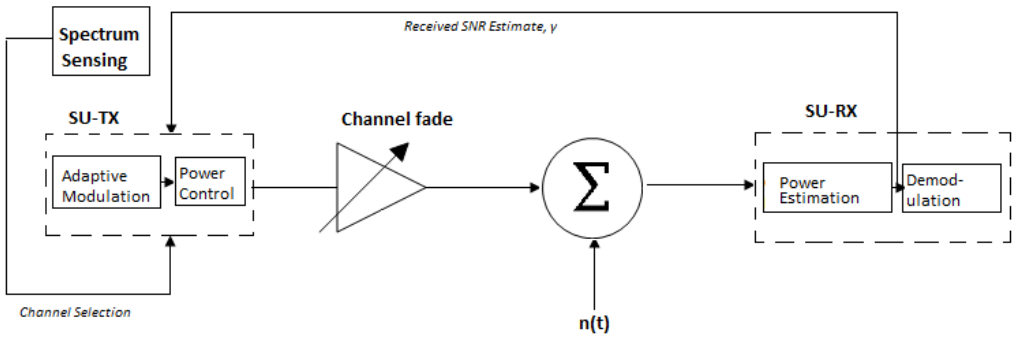

Figure 3.1: Opportunistic Spectrum Access Cognitive Radio Network

fading with Additive White Gaussian Noise, $n(t)$, and noise power spectral density, $\frac{N_0}{2}$. The total system bandwidth B is divided into N channels. Using ideal raised-cosine pulses, each symbol is transmitted within a symbol period, $\frac{N}{B}(1+\alpha)$, where α is the roll-off factor.

3.1 Non-Adaptive Modulation

In this section, we start by looking at the conventional non-adaptive modulation method in OSA CRNs. Given that there is an optimal power control policy implemented, the transmit power is adjusted to compensate for the channel fade, whenever possible while being limited by the peak power, $P_{\max}$. Next, we derive the probability of outage and use it to derive closed form equations for the throughput and bandwidth efficiencies of non-adaptive modulation in OSA CRN.

3.1.1 Outage Probability

A channel outage occurs either if there are no available channels (event A) or if the maximum power needs to be exceeded to maintain the required BER (event B). The probability P_{out} is the probability of a channel outage where no transmission can take place at the required BER and can be broken down as follows,

$$P_{\text{out}} = \Pr\{A \cup B\} = \Pr\{A\} + \Pr\{B\} - \Pr\{A \cap B\}$$

$$P_{\text{out}} = \Pr\{A \cup B\} = \Pr\{A\} + \Pr\{B\} - \Pr\{A\}\Pr\{B\}. \tag{3.1}$$

P_{a} is the probability that a single channel is available. For a modulation scheme requiring at least one channel, $\Pr\{A\}$, the probability that out of N channels none is available, is given by,

$$\Pr\{A\} = (1 - P_{\text{a}})^N . \tag{3.2}$$

In the case where the modulation scheme requires at least one adjacent channel pair, $\Pr\{A\}$, the probability that no adjacent channel pairs are available, is given by,

$$\Pr\{A\} = 1 - \sum_{k=2}^{N} N_{\text{seq}}(k)\, P_{\text{a}}^{k}\, (1 - P_{\text{a}})^{N-k} \tag{3.3}$$

where $N_{\text{seq}}(k)$ is the number of adjacent channel pairs such that there are k available channels in N channels. $N_{\text{seq}}(k)$ may be expressed as,

$$N_{\text{seq}}(k) = \binom{N}{k} - \sum_{j=0}^{min\{k,n-k+1\}} (-1)^{j} \binom{N-k+1}{j} \binom{n-j}{n-k}. \tag{3.4}$$

(3.4) is proven in Appendix C. Given that the transmit power, P_{t}, is Rayleigh distributed, then using the result from (3.5), proven in appendix B, we have in general,

$$\Pr\{P_{\text{t}} > \beta\} = \exp\left(-\frac{\beta}{P_{\text{t}}}\right) \tag{3.5}$$

Therefore we evaluate $\Pr\{B\}$ as,

$$\Pr\{B\} = \Pr\{P_{\text{t}} > P_{\max}\} = \exp\left(-\frac{P_{\max}}{P_{\text{t}}}\right) \tag{3.6}$$

Hence, using results from (3.1), (3.2), (3.5) for modulation schemes requiring one channel slot, the probability of outage, P_{out}, is,

$$P_{\text{out}} = (1 - P_{\text{a}})^{N} + \exp\left(-\frac{P_{\max}}{P_{\text{t}}}\right) - (1 - P_{\text{a}})^{N} \exp\left(-\frac{P_{\max}}{P_{\text{t}}}\right).$$

Using results from equations (3.1), (3.3), (3.5) the probability of outage, P_{out}, for modulation schemes requiring two channel slots is,

$$P_{\text{out}} = \left[1 - \sum_{k=2}^{N} N_{\text{seq}}(k)\, P_{\text{a}}^{k}\, (1 - P_{\text{a}})^{N-k}\right] + \exp\left(-\frac{P_{\max}}{P_{\text{t}}}\right) - \left[1 - \sum_{k=2}^{N} N_{\text{seq}}(k)\, P_{\text{a}}^{k}\, (1 - P_{\text{a}})^{N-k}\right] \exp\left(-\frac{P_{\max}}{P_{\text{t}}}\right). \tag{3.7}$$

3.1.2 Throughput Efficiency

We define the throughput, η, as the ratio of the average data throughput to the instantaneous data rate, $\frac{\bar{R}_b}{R_b}$, expressed as follows,

$$\bar{R_{\mathrm{b}}} = R_{\mathrm{b}} \left[1 - P_{\mathrm{out}}\right]$$

$$\eta = \frac{\bar{R_{\mathrm{b}}}}{R_{\mathrm{b}}} = \left[1 - P_{\mathrm{out}}\right] \tag{3.8}$$

Assuming that the system uses QPSK or 16PSK modulation, $P_{\mathrm{t,QPSK}}$ and $P_{\mathrm{t,16PSK}}$ which are the powers required to maintain the BER if QPSK or 16PSK modulation are employed respectively, can be approximated as follows,

$$P_{\mathrm{t,QPSK}} \approx \frac{P_{\mathrm{t,16PSK}}}{\delta}, \tag{3.9}$$

where δ is 6.5685 (See Appendix B for derivation). Next, we derive the closed form expressions of the throughput of the QPSK and 16PSK modulation schemes. Using (3.8) and the probability of outage for a modulation scheme requiring at least one channel pair as defined by (**??**), we express the QPSK modulation throughput, η_{QPSK}, as,

$$\eta_{\mathrm{QPSK}} = 1 - \left[1 - \sum_{k=2}^{N} N_{\mathrm{seq}}\left(k\right) P_{\mathrm{a}}^{k} \left(1 - P_{\mathrm{a}}\right)^{N-k}\right] - \exp\left(-\frac{P_{\max}}{P_{\mathrm{t,QPSK}}}\right) + \left[1 - \sum_{k=2}^{N} N_{\mathrm{seq}}\left(k\right) P_{\mathrm{a}}^{k} \left(1 - P_{\mathrm{a}}\right)^{N-k}\right] \exp\left(-\frac{P_{\max}}{P_{\mathrm{t,QPSK}}}\right). \tag{3.10}$$

Using (3.8) and the probability of outage for a modulation scheme requiring at least one channel as defined by (3.7), we can express the 16PSK modulation throughput, η_{16PSK} as,

$$\eta_{\mathrm{16PSK}} = 1 - (1 - P_{\mathrm{a}})^{N} - \exp\left(-\frac{P_{\max}}{\delta P_{\mathrm{t,QPSK}}}\right) + (1 - P_{\mathrm{a}})^{N} \exp\left(-\frac{P_{\max}}{\delta P_{\mathrm{t,QPSK}}}\right). \tag{3.11}$$

Bandwidth or spectral efficiency is the ratio of the average throughput in bits/sec to the channel bandwidth in Hertz. In line with the aim of maximizing the spectral efficiency of CRN, we now consider the bandwidth usage of a CRN network when employing either QPSK or 16PSK modulation.

16PSK System

When the system employs 16PSK modulation, transmission occurs if the 16PSK required transmission power is less than $P_{\max}$ and there is at least one channel available. Therefore the average throughput, $\bar{R_{\mathrm{b}}}$, when using 16PSK modulation is,

$$\bar{R_{\mathrm{b}}} = R_{\mathrm{b}} \Pr\{P_{\mathrm{t,16PSK}} < P_{\max}\} \Pr\{\text{At Least One Channel Available}\}, \tag{3.12}$$

The bandwidth, B, can be expressed as,

$$B = R_{\mathrm{s}}\,(1+\alpha) \tag{3.13}$$

$$= \frac{R_{\mathrm{b}}}{\log_2(M)}\,(1+\alpha) \tag{3.14}$$

$$= \frac{R_{\mathrm{b}}}{\log_2(16)}\,(1+\alpha)\,, \tag{3.15}$$

where R_{b} is the instantaneous bit rate, M is the modulation order or the number of symbols on the constellation and α is the roll-off factor. $M = 16$ when 16PSK modulation is employed. Hence

$$B = \frac{R_{\mathrm{b}}}{4}\,(1+\alpha) \tag{3.16}$$

$$R_{\mathrm{b}} = \frac{4B}{1+\alpha}. \tag{3.17}$$

Simplifying (3.12) using (3.17) we get

$$\bar{R_{\mathrm{b}}} = \frac{4B}{1+\alpha}\Pr\{P_{\mathrm{t,16PSK}} < P_{\max}\}\Pr\{\text{At Least One Channel Available}\}, \tag{3.18}$$

Using (3.2) and (3.5), we evaluate the probability that at least one channel is available and the probability that the required transmission power, when 16PSK modulation is employed, is less than $P_{\max}$. We then substitute them in (3.18) to compute the bandwidth efficiency of the 16PSK modulation scheme, η_{B16PSK},

$$\eta_{\mathrm{B16PSK}} = \frac{\bar{R_{\mathrm{b}}}}{B} = \left(\frac{4}{1+\alpha}\right)\left[1-\exp\left(\frac{-P_{\max}}{P_{\mathrm{t,16PSK}}}\right)\right]\left[1-(1-P_{\mathrm{a}})^N\right]. \tag{3.19}$$

QPSK system

When the system employs QPSK modulation, transmission occurs when the required transmission power is less than $P_{\max}$ and there are at least two adjacent channel slots available. Therefore,

$$\bar{R_{\mathrm{b}}} = R_{\mathrm{b}}\Pr\{P_{\mathrm{t,QPSK}} < P_{\max}\}\Pr\{\text{At Least One Channel Pair Available}\}. \tag{3.20}$$

QPSK modulation scheme has four symbols in the constellation, hence $M = 4$. Using (3.13), the instantaneous bit rate, R_{b} can be expressed as,

$$R_{\mathrm{b}} = \frac{2B}{1+\alpha}, \tag{3.21}$$

$$\Pr\{\text{At Least One Channel Pair Available}\} \quad = \quad \sum_{k=2}^{N} N_{\text{seq}}(k) P_{\text{a}}^{k} (1-P_{\text{a}})^{N-k}. \quad (3.22)$$

Simplifying further, using (3.22) and (3.4) proven in appendix C, results in,

$$\eta_{\text{BQPSK}} = \frac{\bar{R}_{\text{b}}}{B} = \left[\frac{2}{(1+\alpha)} \sum_{k=2}^{N} N_{\text{seq}}(k) P_{\text{a}}^{k} (1-P_{\text{a}})^{N-k}\right] \left[1 - \exp\left(\frac{-P_{\max}}{P_{\text{t,QPSK}}}\right)\right], \quad (3.23)$$

where η_{BQPSK} is a fundamental parameter to gauge the spectral efficiency of the system, when QPSK modulation is employed.

3.2 Adaptive Modulation

In this section, we look at the CRN system, as it implements adaptive modulation, switching from the less robust 16PSK to the more robust modulation scheme, QPSK, during deep fades. To maintain the same data rate as we drop from 4 bits per symbol to 2 bits per symbol, the symbol rate increases when switching from 16PSK to QPSK modulation. This modulation shift requires twice the bandwidth, or two adjacent channel slots. Bearing this in mind, we derive closed form expressions for the throughput and bandwidth efficiencies when the adaptive modulation technique is employed.

3.2.1 Outage Probability

No data transmission occurs when there is enough required transmit power, $P_{\text{t,16PSK}}$, to close the 16PSK link but there are no channels available. When the system is operating in QPSK mode and the transmit power, $P_{\text{t,QPSK}}$, is within the acceptable range ($\frac{P_{\max}}{\delta} < P_{\text{t,QPSK}} < P_{\max}$) but no adjacent channel pair is available, then no data transmission occurs. Finally, if the system requires a QPSK transmission power higher than the regulatory $P_{\max}$ to maintain the BER, then transmission is halted. Therefore, putting these three cases together, the probability of outage, P_{out}, is,

$$\begin{aligned} P_{\text{out}} = {} & \Pr\{P_{\text{t,16PSK}} < P_{\max}\} \Pr\{\text{No Channels Available}\} \\ & + \Pr\{\frac{P_{\max}}{\delta} < P_{\text{t,QPSK}} < P_{\max}\} \Pr\{\text{No Channel Pair Available}\} \\ & + \Pr\{P_{\text{t,QPSK}} > P_{\max}\}. \end{aligned} \quad (3.24)$$

Evaluating each probability term,

$$\Pr\{\text{No Channels Available}\} = (1 - P_{\text{a}})^N , \tag{3.25}$$

$$\Pr\{\text{No Channel Pair Available}\} = 1 - \sum_{k=2}^{N} N_{\text{seq}}(k)\, P_{\text{a}}^k\, (1 - P_{\text{a}})^{N-k} \tag{3.26}$$

Recall that P_{a} was defined as the probability that a single channel is available and $N_{\text{seq}}(\text{k})$ is defined in (3.4). Similarly to the previous section, there are N channels available, and the probability that a channel is not available is easily derived as (3.25). Moreover, the probability that an adjacent channel pair is not available is given by (3.26). Combining (3.5) and (3.9) results in,

$$\Pr\{P_{\text{t,16PSK}} < P_{\max}\} = \Pr\{P_{\text{t,QPSK}} < \frac{P_{\max}}{\delta}\} = 1 - \exp\left(-\frac{P_{\max}}{\delta P_{\text{t,QPSK}}}\right)$$

and,

$$\Pr\{\frac{P_{\max}}{\delta} < P_{\text{t,QPSK}} < P_{\max}\} = \exp\left(-\frac{P_{\max}}{\delta P_{\text{t,QPSK}}}\right) - \exp\left(-\frac{P_{\max}}{P_{\text{t,QPSK}}}\right) \tag{3.27}$$

$$\Pr\{P_{\text{t,QPSK}} > P_{\max}\} = \exp\left(-\frac{P_{\max}}{P_{\text{t,QPSK}}}\right) \tag{3.28}$$

Evaluating P_{out} from (3.24) using the above terms results in,

$$P_{out} = \left[1 - \exp\left(-\frac{P_{\max}}{\delta P_{\text{t,QPSK}}}\right)\right]\left[(1 - P_{\text{a}})^N\right] + \left[\exp\left(-\frac{P_{\max}}{\delta P_{\text{t,QPSK}}}\right) - \exp\left(-\frac{P_{\max}}{P_{\text{t,QPSK}}}\right)\right] \left[1 - \sum_{k=2}^{N} N_{\text{seq}}(k)\, P_{\text{a}}^k\, (1 - P_{\text{a}})^{N-k}\right] + \exp\left(-\frac{P_{\max}}{P_{\text{t,QPSK}}}\right). \tag{3.29}$$

3.2.2 Throughput Efficiency

We now derive a closed form equation of the throughput efficiency, η, for the adaptive modulation case using (3.8) and (3.29). The throughput efficiency, η, is given by,

$$\eta = 1 - P_{\text{out}} \tag{3.30}$$

$$\eta = 1 - \left[1 - \exp\left(-\frac{P_{\max}}{\delta P_{\text{t,QPSK}}}\right)\right]\left[(1 - P_{\text{a}})^N\right] - \left[\exp\left(-\frac{P_{\max}}{\delta P_{\text{t,QPSK}}}\right) - \exp\left(-\frac{P_{\max}}{P_{\text{t,QPSK}}}\right)\right] \left[\sum_{k=2}^{N} N_{\text{seq}}(k)\, P_{\text{a}}^k\, (1 - P_{\text{a}})^{N-k}\right] - \exp\left(-\frac{P_{\max}}{P_{\text{t,QPSK}}}\right) \tag{3.31}$$

3.2.3 Bandwidth Efficiency

Next, we consider the bandwidth efficiency of an MPSK adaptive system, employing QPSK and 16PSK modulation. We base the following derivations on the assumptions that if the transmission power is greater than or equal to $P_{\max}$, transmission is halted and the BER degrades. This is important because the SU cannot exceed the regulatory peak power, $P_{\max}$. To start with, the bandwidth efficiency is defined as the ratio of the maximum throughput to the bandwidth of a communication channel. More precisely, using (3.12),

$$B = \frac{R_{\mathrm{b}}\,(1+\alpha)}{\log_2\,(M)} \tag{3.32}$$

where M is the modulation order, R_{b} is the instantaneous bit rate and and α is the roll-off factor. The instantaneous data rates for the 16PSK and QPSK modulation scheme can hence be defined, respectively, as,

$$R_{\mathrm{b}} = \frac{4B}{(1+\alpha)}, \quad \text{for} \quad \text{16PSK} \tag{3.33}$$

$$R_{\mathrm{b}} = \frac{2B}{(1+\alpha)}, \quad \text{for} \quad \text{QPSK} \tag{3.34}$$

The average throughput, $\bar{R}_{\mathrm{b}}$, in the adaptive system switching between QPSK and 16PSK modulation can be expressed as,

$$\begin{aligned}\bar{R}_{\mathrm{b}} = &\left[\frac{4B}{1+\alpha} Pr\{P_{\mathrm{t,16PSK}} < P_{\max}\}\right] \Pr\{\text{At Least One Channel Available}\} \\ &+ \left[\frac{2B}{1+\alpha} \Pr\{P_{\mathrm{t,16PSK}} > P_{\max}\}\right] \Pr\{\text{At Least One Channel Pair Available}\}\end{aligned} \tag{3.35}$$

Using (3.5), (3.27) and (3.33), the bandwidth efficiency, $\eta_B = \frac{\bar{R}_{\mathrm{b}}}{B}$, is given by,

$$\begin{aligned}\eta_{\mathrm{B}} = &\frac{4}{1+\alpha}\left[1 - \exp\left(\frac{-P_{\max}}{P_{\mathrm{t,16PSK}}}\right)\right] \Pr\{\text{At Least One Channel Available}\} \\ &+ \left[\frac{2}{1+\alpha} \exp\left(\frac{-P_{\max}}{P_{\mathrm{t,16PSK}}}\right)\right] \Pr\{\text{At Least One Channel Pair Available}\}\end{aligned} \tag{3.36}$$

Further evaluating, using (3.9), (3.25), (3.26), yields a bandwidth efficiency for the adaptive case of,

$$\eta_{\mathrm{B}} = \frac{4}{1+\alpha}\left[1-\exp\left(\frac{-P_{\max}}{P_{\mathrm{t,QPSK}}}\right)\right]\left(1-(1-P_{\mathrm{a}})^{N}\right) + \frac{2}{1+\alpha}\exp\left(\frac{-P_{\max}}{P_{\mathrm{t,QPSK}}}\right)\sum_{k=2}^{N} N_{\mathrm{seq}}(k)\, P_{\mathrm{a}}^{k}\,(1-P_{\mathrm{a}})^{N-k} \quad (3.37)$$

3.3 Numerical Results & Discussion

In the following figures, we depict the spectral efficiency for OSA CRNs. More specifically, the first three figures, Figs 3.2, 3.3 and 3.4 depict the spectral efficiency for adaptive MPSK and non-adaptive QPSK in bits/sec/Hz versus the ratio of the maximum transmit power, $P_{\max}$, to the average required QPSK transmission power, $P_{\mathrm{t,QPSK}}$, in OSA CRNs. The roll-off factor, α is set to 0.4. To start with, Fig. 3.2 illustrates the gain in bandwidth efficiency as the number of channels, N, increases in both adaptive and non-adaptive cases, although adaptive case, show a marked improvement as N increases, compared to the non-adaptive case which still gives a performance much less than 0.5 bits/sec/Hz for $N = 16$. On the other hand, even for the lowest number of channels, $N = 2$, the adaptive MPSK's performance is much better than the non-adaptive QPSK modulation with $N = 2$. With increasing probability of an available channel, P_{a}, there is a noticeable bandwidth efficiency performance gain for both adaptive MPSK and non-adaptive QPSK, and the interesting feature to note is that the bandwidth efficiency saturates, as N increases, in high P_{a}; For example, in Figs 3.3 and 3.4, the curves for $N = 8$ and $N = 16$ in the adaptive case overlap, mainly because, with high P_{a}, the probability of finding an adjacent channel pair to switch to QPSK mode to counteract deep fades is higher. Overall, the graphs for adaptive MPSK show a decrease in performance as $P_{\max}/P_{\mathrm{t,QPSK}}$ tends to 1. This can be explained by the fact that, when the $P_{\mathrm{t,QPSK}}$ is high, hence the lower ratio, $P_{\max}/P_{\mathrm{t,QPSK}}$, is the same as a lower received instantaneous SNR value, γ. Upon detecting a lower γ, the system switches to QPSK to compensate for the channel fade and meet the required BER. Since QPSK is less bandwidth efficient than 16PSK modulation, the BER requirement is met at the expense of bandwidth.

The throughput efficiency graphs, Figs 3.5, 3.6 and 3.7, exhibit similar behaviour, demonstrating the markedly higher performance of adaptive MPSK as N increases. It is interesting to note, similarly to the bandwidth efficiency graphs that the throughput efficiency also saturates for high value of N and P_a, since the probability of establishing a 16PSK link is higher and also the probability of finding a channel pair to switch to QPSK modulation in deep fades is significantly higher. The general trend of decreasing throughput efficiency with higher average required transmission power is to be expected. As the system requires a high average power to maintain the BER, which means that there is a lower detected SNR, γ, at the receiver, the system switches to QPSK more often. The QPSK modulation scheme transmits lower number of bits per symbol than the 16PSK modulation scheme, explaining the lower throughput performance. Both bandwidth and

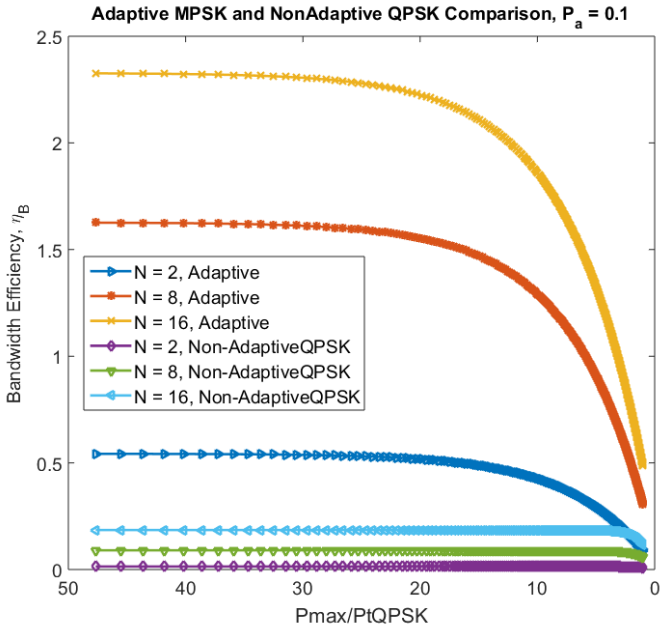

Figure 3.2: Bandwidth Efficiency for adaptive and non adaptive MPSK, given a probability available channel of $P_{\mathrm{a}} = 0.1$

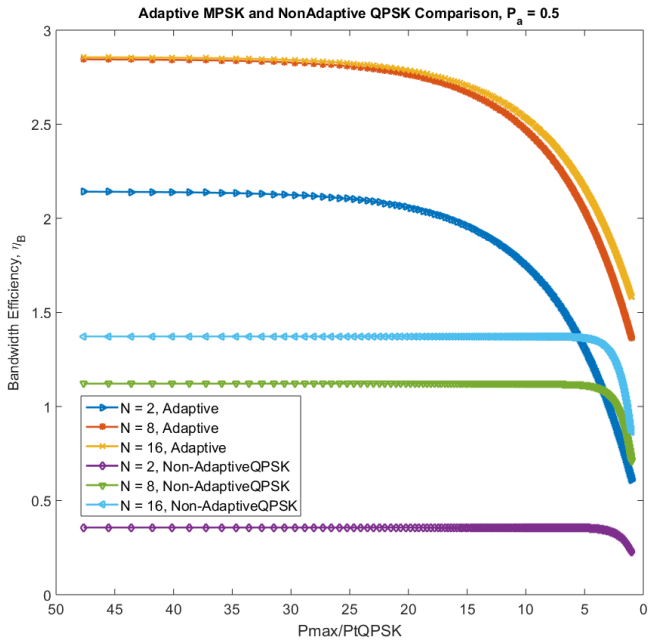

Figure 3.3: Bandwidth Efficiency for adaptive and non adaptive MPSK, given a probability available channel of $P_{\mathrm{a}} = 0.5$

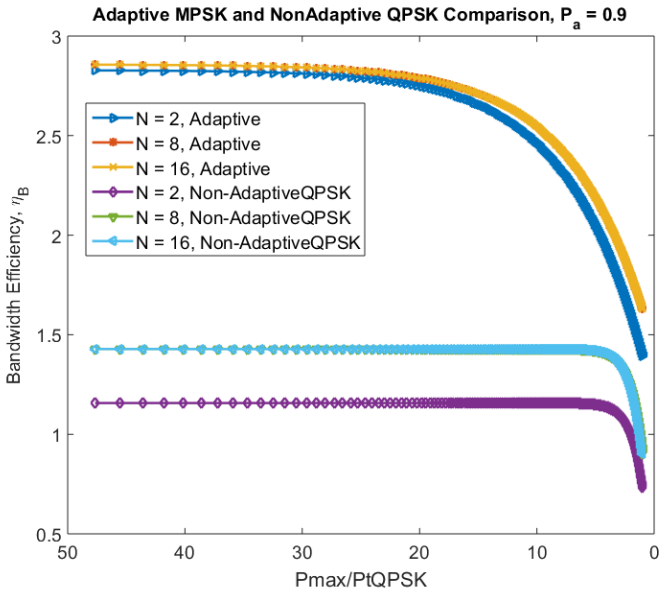

Figure 3.4: Bandwidth Efficiency for adaptive and non adaptive MPSK, given a probability available channel of $P_{\mathrm{a}} = 0.9$

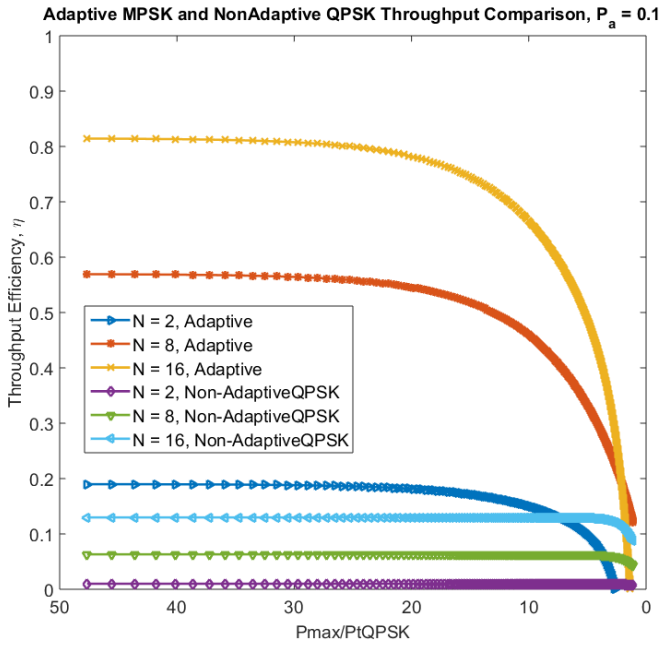

Figure 3.5: Throughput Efficiency for adaptive and non adaptive MPSK, given the probability of an available channel of $P_{\mathrm{a}} = 0.1$

throughput efficiency graphs exhibit significant performance gain in the MPSK adaptive modulation case compared to non-adaptive QPSK in an OSA CRN, with optimal power

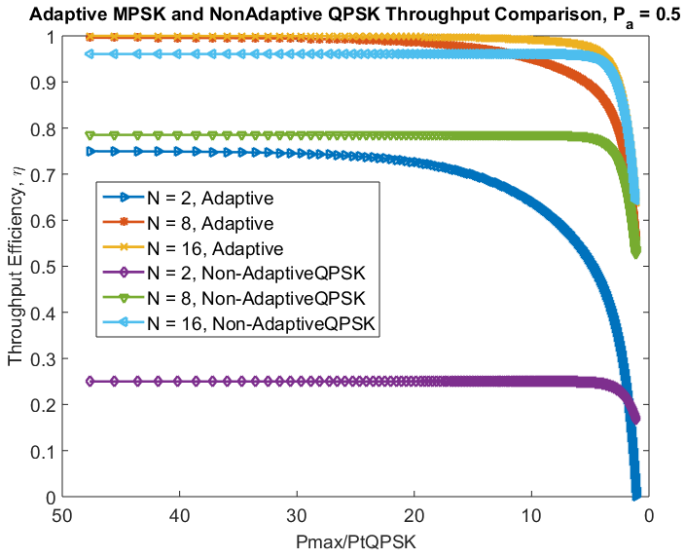

Figure 3.6: Throughput Efficiency for adaptive and non adaptive MPSK, given the probability of an available channel of $P_{\mathrm{a}} = 0.5$

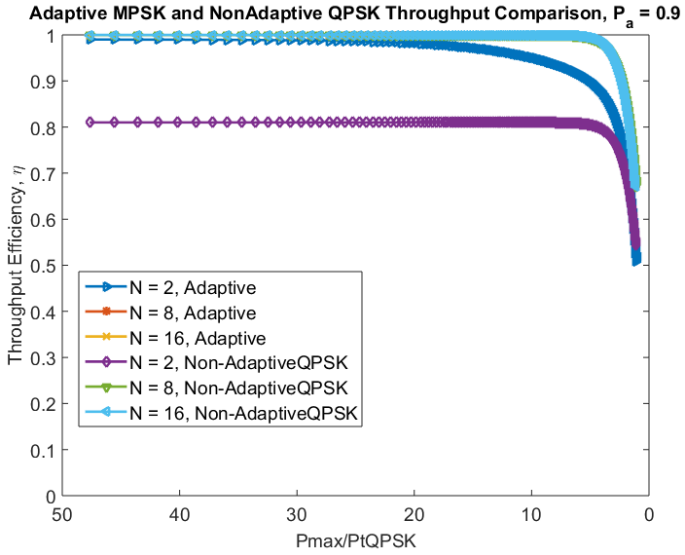

Figure 3.7: Throughput Efficiency for adaptive and non adaptive MPSK, given the probability of available channel of $P_{\mathrm{a}} = 0.9$

control techniques. Having analytically proven the benefits of adaptive techniques in CRN, we now proceed in designing and developing simulations in MATLAB to verify, in the next chapter.

Chapter 4

Simulation Models Design And Development

In this chapter, we now proceed to develop the adaptive modulation simulation model. In the study of communication systems, the classical AWGN channel with statistically independent free of intersymbol interference (ISI), is the usual starting point for understanding basic performance relationships" [37]. To start with, we started building a basic QPSK over AWGN simulation. The Appendix A has a complete derivation of the discrete time representation of the system and noise variance. We then build on the AWGN simulation to include Jakes Flat Fading time-varying channel. We designed a Jakes Filter which we used to obtain fade coefficients and convolve with the signal vector. Having completed this, we investigated thoroughly many SNR estimators and implemented EVB moments-based one suitable for MPSK modulation schemes. We then developed the MPSK modulator, demodulator and finally conducted experiments for slow and very fast Rayleigh fading.

4.1 MATLAB Coding

In this section, the essential parts of the codes developed to simulate the AWGN model and the complete code is given in Appendix A. The program generates a random set of 512 bits and loop through 8 times to calculate a BER value for each of the 8 "Eb_No" values. Note the variable "iiEbNo" has been made the loop variable to repeat the same steps of passing the 512 bits, creating signal vector, adding noise, demodulate and calculate the BER of each "Eb_No". The Number of samples per baud variable is Nspb = 16 and the number, N is the number of bit errors that we would like the loop to repeat itself until a certain number of errors have been obtained. This gives an accurate result due to the simple reason as taking a higher statistical sample gives a better accuracy and portrayal of the actual situation. N is thus 1000 in this case which is sufficient for an accurate measure of the BER.

```
Eb_No_dB=[0:1:7]; %Eb/No
```

```
N=1000;%The number of bit errors for the error determination
blocklength=512;%The bit error rate is obtained in blocks of data
Nspb=16;
```

As we start, the variables, number of errors and number of bits are set to zero. Number of bits variable will be incrementing by a factor of 512 for each loop, while the number of errors will count the number of errors in each loop and add them incrementally. The variable, "sigma_n" is as derived in above sections and setting A to be 1 since it can be arbitrary, we get:

$$\sigma_{\tilde{n}} = \sqrt{\frac{N_{SPB}}{4\frac{E_b}{N_0}}} \tag{4.1}$$

```
N_errors=0;     %Number of bit errors counter
N_bits=0;       %Number of bits counter
sigma_n=sqrt(Nspb/(4*Eb_No(iiEbNo))); %Noise Standard Deviation
condition=0; %N bit errors not yet obtained
```

At this point the program checks the status of the "condition" variable. Initially, it will enter this loop as the variable is preset to zero and will be in this loop till the number of errors is greater than the value N which holds the preset number of errors required. For each loop, the number of bits is incremented by the number of bits passed to the loop, that is, for each loop a blocklength of 512 is being added.

```
N_bits=N_bits+blocklength;
```

The data block of size blocklength is then generated by using the "randn" function which produces 512 Gaussian random variables

```
data=randn(1,blocklength); %Generated random binary data
```

Since information is sent in binary that is only zeros and ones, we iterate through each variable in the data vector and assign it to be either 1 or 0. If the data is greater than zero, it is set to 1 else it is set to 0. We then successfully form a vector of 256 bits of zeros and ones.

```
for ii=1:blocklength
            if data(ii)>0
                data(ii)=1;
            else
                data(ii)=0;
            end
end
```

In QPSK each symbol, or pair of bits, is recognised by its phase. So we have to take the data vector and assign each pair of bits or symbol to a phase value. The pair is defined as "a" and "b" and they are four possible bit combinations $00, 10, 11, 01$ which are mapped to a specific phase value $\left\{\frac{\pi}{4}, \frac{3\pi}{4}, \frac{5\pi}{4}, \frac{7\pi}{4}\right\}$ respectively to finally form the phase vector phi which will contain 256 symbols' phases (as the blocklength is 512 and 2 bits form a symbol in QPSK).

```
for ii=1:2:blocklength   %Generate QPSK phases
            a=data(ii);
            b=data(ii+1);
            if a==0 & b==0
                phi(ii/2+1/2)=pi/4;
            elseif a==1 & b==0
                phi(ii/2+1/2)=3*pi/4;
            elseif a==1 & b==1
                phi(ii/2+1/2)=5*pi/4;
            else
                phi(ii/2+1/2)=7*pi/4;
            end
end
```

Now, we generate the noise vector "n", by inputting the variables "Eb_No" and "sigma_n" as parameters. "Nspb" is 16 and "blocklength/2" is 512 which makes it a vector of 4096 elements. The value of "sigma_n" calculated using the particular "Eb_No" value will make the average noise energy to be equal to "Eb_No".

```
n=sigma_n.*(randn(1,Nspb*blocklength/2)+j*randn(1,Nspb*blocklength/2));
```

We now produce the signal vector "s" for the block of 256 symbols by iterating through "N_samples", and for each symbol we iterate through "Nspb" samples and assign each sample the value corresponding to the value $e^{j\varphi}$ where φ. The iteration will go for 256 times, and the inner loop iterates for 16 times for each symbol since "Nspb" samples is 16.

```
for ii=1:blocklength/2 %Generate signal vector for the block
            s((ii-1)*Nspb+1:(ii*Nspb))=exp(j*phi(ii)).*ones(1,Nspb);
end
```

The AWGN channel is nothing but the effects of noise on the signal, hence the addition of the signal vector to noise vector below.

```
r=s+n; %Additive Communications Channel
```

Demodulation occurs by iterating through the "r", 256 times, since we have 256 symbols, and at each iteration the sum of the 16 samples which represent a particular symbol is computed. "r" being a complex value has a real and imaginary part or more precisely, the Quadrature (real) and Imaginary part. The variable "u" stores the sum of the real part while the variable "v" stores sum obtained for the imaginary part. Now the bit detection occurs as follows, if the sum of the real part is greater than zero then the new vector "datar", denoting data received, stores a value of zero else a value of 1 is saved. Same goes for the imaginary part. The two dimensional vector datar will save the value received for pair of bits forming a symbol.

```
for ii=1:blocklength/2  %Symbol detection
            u=real(sum(r((ii-1)*Nspb+1:(ii*Nspb))));
            v=imag(sum(r((ii-1)*Nspb+1:(ii*Nspb))));
            iir=iir+1;
            %bit detection
            if u>=0
                datar(iir)=0;
            else
                datar(iir)=1;
            end
            iir=iir+1;
            if v>=0
                datar(iir)=0;
            else
                datar(iir)=1;
            end
end
```

Having the transmitted data and the received data in two vectors we now compute the number of errors by checking for similarity. Since this is in binary, 0 and 1's we can easily harness the power of 'mod' function here. As we go along and sum each bit from the two vectors, we know that summing two zeros or two ones give an even number. Hence if it is identical, which means no errors, there are no errors while if there is an error, the remainder is 1 and the error number is incremented by 1.

```
errornumber=sum(mod((data+datar),2)); %Number of bit errors in block
```

Add the number of bit errors just computed above in that loop and checking whether we have exceeded the preset value of 1000 already. If not we go in another loop and repeat.

```
N_errors=N_errors+errornumber; %Total number of bit errors
        if N_errors>N
            condition=1;
        end
```

Using the Monte Carlo method, we find "PB" by doing; total number of bit errors divided by the total number of bits transmitted

```
PB(iiEbNo)=N_errors/N_bits   %bit error rate estimate
```

We then plot and analyse the results.

```
PB_theory=qfunc(sqrt(2*Eb_No));
```

Refer to Appendix B for the complete program.

4.2 Jakes Flat Fading Time Varying System

This code was built on the AWGN model, hence it is a QPSK Monte Carlo simulation as well, using matched filter detection as above. However, to simulate Rayleigh Fading, we constructed a Jakes Filter, that we spectrally shape a Jakes filter to obtain the spectrum and compute the fade coefficients. We will go through the essential parts of the program only. We start with defining the "Eb_No_dB" vector for which probability bit error will be computed and plotted. Most other variables, "blocklength",“ Nspb", "N", carry same function as above AWGN channel case. "v_km_hr is the speed in kilometres per hour and "v" converts it to metres/sec. "f0" is the transmitting frequency, "Rb" is the data rate in bits per second and "fs" is the sample rate which is a function of data rate and "Nspb". Another new variable here is the Doppler frequency which is a function of the velocity of the moving receiver, transmit frequency and speed of light.

```
Eb_No_dB=[-2:1:14] ;   %Eb/No
N=50000;  % The number of bit errors for the error determination
blocklength=4096;  % The bit error rate is obtained in blocks of data
Nspb=16;
v_km_hr=110;% v_km_hr is the velocity in km/hr
v=v_km_hr*1000/3600; % v is the velocityt in m/sec
fo=900.e6; % fo is the transmit frequency in Hertz
c=3.e8; % c is the speed of light in m/sec
fD=v*fo/c; % fD is the Doppler frequency in Hertz
Rb=14.e3; % Rb is the bit rate in bits/s
fs=Rb*Nspb; %fs is the sample rate in samples/s
```

This piece of code is generating the Jakes Power Spectral Density (PSD) represented by the following equation:

$$s(f) = \frac{1}{\pi f_d \sqrt{1 - (\frac{f}{f_d})^2}}, |f| \leq f_d \tag{4.2}$$

Note that the constant π x f_d has been omitted from the denominator in the actual Jakes PSD construction because later the values will be normalised and any constants would be removed anyway.

```
for k=N_samples/2+1:N_samples
    m=k-N_samples/2-1;
    if abs(m*fs/N_samples)<fD
        SyI1(k)=1./sqrt(1-(m*fs/(N_samples*fD)).^2);
    else
        SyI1(k)=0;
    end
end
for k=1:N_samples/2
    m=k-N_samples/2-1;
    if abs(m*fs/N_samples)<fD
        SyI1(k)=1./sqrt(1-(m*fs/(N_samples*fD)).^2);
    else
        SyI1(k)=0;
    end
end
for k=1:N_samples
    freq(k)=(-N_samples/2-1+k)*fs./N_samples;
end
```

This piece of code shows how the the Doppler Filter transfer function is found by taking the square root of the Jakes Power Spectral Density. This can be justified by this equation, quoted from the book [38].

$$S_d(f) = S_{\tilde{n}\tilde{n}}(f)|\tilde{H}(f)|^2 = |\tilde{H}(f)|^2 \tag{4.3}$$

Where, S_d is the Jakes Power Spectral Density, $S_{\tilde{n}\tilde{n}}$ is the Noise Power Spectral Density. The Doppler filter can be spectrally shaped by passing white Gaussian noise through a Gaussian filter having transfer function H. However we have already constructed the Jakes PSD. To obtain the Doppler filter we do:

$$\tilde{H}(f)^2 = \sqrt{S_d(f)} \tag{4.4}$$

The remaining codes are just to plot and view the plots of the PSD and Doppler filter

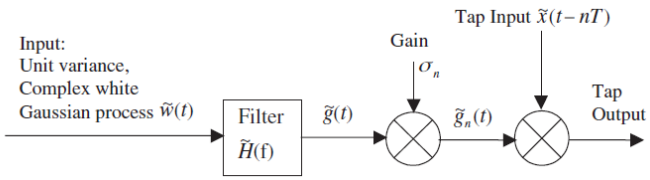

Figure 4.1: Generating tap gain processes

```
figure(1)
plot(freq, abs(SyI1))
title('SyI1(f), power spectral density of the signal envelope')
xlabel('frequency (Hertz)')
ylabel('S_y_I1(f)')
axis([-10*fD 10*fD 0 max(SyI1)])
grid
H=sqrt(SyI1);
figure(2)
plot(freq,H)
axis([-10.*fD 10*fD 0 max(H)])
grid
xlabel('frequency (Hz)')
ylabel('|H(f)|')
title('|H(f)| as a function of frequency')
H=fftshift(H);

Eb_No=10.^(Eb_No_dB./10);
for iiEbNo=1:length(Eb_No);
    N_errors=0;      % Counter for the number of bit errors
    N_bits=0;        % Counter for the number of bits
    sigma_n=sqrt(Nspb/(4*Eb_No(iiEbNo))); % Noise standard deviation
    condition=0;   % N bit errors not yet obtained
```

The above code is initalisation of variables similar to the AWGN case. However the following codes are specific to this Jakes Raleigh model. Since it is flat fading, we have only 1 tap and 1 tap gain process to generate and that's what we are doing below. See Fig 4.1, it shows how white Gaussian noise is passed through the Doppler filter to generate the tap processes gain and the latter is then normalised to 1. This normalisation take place so that we can scale the noise to have an average "Eb_No".

```
    while condition==0
        N_fade=H.*fft(randn(1,N_samples)+j.*randn(1,N_samples));
        n_fade=ifft(N_fade);
        n_fade_env=abs(n_fade);
```

```
% Average Power in the Fade
P_n_fade=sum(n_fade_env.*n_fade_env)./N_samples;
% Scale to unity average power in the Fade
n_fade_env=n_fade_env/sqrt(P_n_fade);
```

Then later in the code, we come to the point where we multiply the fade envelope with the signal vector to finally obtain the faded signal as an output. Important thing to note here is that the simulation assumes that the multi-path induced phase variations in the received signal are tracked out by the carrier taking loop. Therefore only variation in the envelope of the signal need to be modelled in the simulation.

```
for kk=1:N_samples
    x(kk)=x(kk).*n_fade_env(kk);
end
```

We finally add noise to the faded envelope which is the received signal y. The later processes are similar to the AGWN case where there is matched filter detection and Monte Carlo PB calculation.

```
y=x+n;  % Additive Communications Channel
```

4.3 Adaptive Modulation Components

The above codes and derivation are for a basic QPSK system over AWGN and Rayleigh channel. However, the modulator and demodulator was designed to accommodate MPSK signals. The Jakes filter was also modified into a more robust one. In addition, two different SNR estimators was implemented, as will be explained in the following sections

4.3.1 MPSK Modulator

The MPSK modulator works by first reshaping the data into 'M' number of columns. For example a blocklength of 6000 bits, for an 8PSK system will be 3 x 2000 matrix. Then the constellation is created, with a set of bits representing each symbol assigned to a constellation. Finally the block of data is assigned to a constellation and a signal vector is generated.

```
data1 = reshape(data,NobitsPerSymbol,blocklength/NobitsPerSymbol);
       jval = (0:M-1)';
       mapping = bitxor(jval,bitshift(jval,-1));
       bitmap=deci2bin(mapping',NobitsPerSymbol);
       symbolmapping=[(0:M-1)' bitmap];
       si = exp(j.*2.*pi./M.*(0:M-1)');

       for iPhase = 1:size(si)
```

```
            siPhases(iPhase) = atan2(imag(si(iPhase)),real(si(iPhase)));
            siPhasesOne(iPhase) = siPhases(iPhase);
            if siPhases(iPhase) < 0
                siPhases(iPhase) = siPhases(iPhase) + 2*pi;
            end
            if siPhases(iPhase) == 0
                siPhasesOne(iPhase) = 2*pi;
            end
        end
        s=zeros(1,length(data1));
        sd=zeros(1,length(data1));
        for counter=1:size(data1,2),
            mData=data1(1:NobitsPerSymbol,counter)';
            for counter2=1:M,
                if mData== symbolmapping(counter2,2:end),...
                sd(counter)=symbolmapping(counter2,1);...
                s(counter)=exp(j.*2.*pi./M.*symbolmapping(counter2,1));
                end
            end
        end
```

4.3.2 Demodulator

The demodulator is part of the matched filtering process, which also calculates the phase of the received symbol and do a one-to-one mapping from the constellation and retrieve the symbols back and save it in a vector. Later, the original and received bit streams are compared for discrepancies.

```
  for ii=1:blocklength/NobitsPerSymbol   % Symbol detection
              u=real(sum(y((ii-1)*Nspb+1:(ii*Nspb))));
               v=imag(sum(y((ii-1)*Nspb+1:(ii*Nspb))));
                 Sym_detected_phase = atan2(v,u);
                 if Sym_detected_phase < 0
                     Sym_detected_phase = Sym_detected_phase + 2*pi;
                 end
                 Sym_detected_phase = mod(Sym_detected_phase,2*pi);
                 [c index] = min(abs(siPhases - Sym_detected_phase));
                 [d index1] = min(abs(siPhasesOne - Sym_detected_phase));
                 if c < d
                     detectedSymbol = symbolmapping(index,2:end);
                 else
```

```
            detectedSymbol = symbolmapping(index1,2:end);
        end
        for iiter = 1:NobitsPerSymbol
            datar(iiter+iir) = detectedSymbol(iiter);
        end
        iir = iir + NobitsPerSymbol;
    end
```

4.3.3 SNR estimator

M2M4 EVB estimator

Since the estimator in [22] was defined in the time domain, we worked out the equivalence of the derived formula to work with the complex envelope. To compute the SNR estimate using the M2M4 estimator, we have to calculate the moments of the received symbols, for both the real and imaginary components(m_two_r,m_four_r,m_two_i,m_four_r). We then used a polynomial fit tool in MATLAB to derive a curve fit for each PSK modulation scheme which we use to compute SNR for both real and imaginary components. Eventually we averaged those two values to get the final SNR estimate.

```
m_two_r =  mean((abs(real(R))).^2); m_four_r = mean((abs(real(R))).^4);
m_two_i =  mean((abs(imag(R))).^2); m_four_i = mean((abs(imag(R))).^4);
z_hat_real(iEbNo,n)=z_hat_r;    z_hat_imag(iEbNo,n)=z_hat_i;
 Eb_No_est_dB_r(iEbNo)=P_r(1).*z_hat_r.^4 +P_r(2).*z_hat_r.^3....
 +P_r(3).*z_hat_r.^2 + P_r(4).*z_hat_r +P_r(5);
  Eb_No_est_dB_i(iEbNo)=P_i(1).*z_hat_i.^4 +P_i(2).*z_hat_i.^3+...
  P_i(3).*z_hat_i.^2 + P_i(4).*z_hat_i +P_i(5);
Eb_No_est_dB(iEbNo) = (Eb_No_est_dB_r(iEbNo) + Eb_No_est_dB_i(iEbNo))./2;
```

QPSK_Real	QPSK_Imag	8PSK_Real	8PSK_Imag	16PSK_Real	16PSK_Imag
898.602831	898.602831	24795.9584	28168.7641	25971.889	19628.08518
-1800.6247	-1800.62469	-270548.49	-307304.36	-283777.97	-214679.6245
1314.90879	1314.90879	1106830.9	1257005.65	1162572.54	880420.2291
-394.902	-394.901996	-2012265.2	-2284903.6	-2116521	-1604623.097
41.6871882	41.6871882	1371770.7	1557341.61	1444806.91	1096645.705

Figure 4.2: Polynomial curve fit coefficients for real and Imaginary components

4.4 Conclusion

The key factor in getting this to function properly was working out how to make the estimator work for the complex envelope since it was designed, primarily for the time domain, in contrast to our simulation working with complex envelope. Having designed, developed and tested each components for the adaptive modulation, we then ran experiments analysed the result, described in next chapters.

Chapter 5

Results

Over the last chapters, we have introduced basic concepts of cognitive radio, adaptive modulation techniques, SNR monitoring techniques and explained how the models were devised including the assumptions made. A cognitive radio model was described and in the same breath, Rayleigh fading channel model was implemented to observe how adaptive modulation can contribute to the overall improvement of BER, power and spectral efficiency in a cognitive radio system. There are quite a few papers,where significant research have been conducted, mainly by Alouini, Goldsmith [16] [10] among others, though their model primarily assumed a slow fading scenario, where the coherence time is greater than the symbol time, which means fading is constant across few symbols. In the course of project, we not only investigated slow Rayleigh fading but also very fast fading, where fading occurs within symbol time. A substantial amount of time also went into investigating and implementing many different SNR estimators, to eventually find a suitable one for the purpose of this project. The following sections will go through the results of the simulations conducted, starting by the basic AWGN channel over QPSK, the flat fading Rayleigh model implemented using a jakes Doppler filter to adaptive modulation performance over slow fading and very fast fading Rayleigh channels.

5.1 AWGN Channel Over QPSK

This is the simplest model implemented to study the effects of Gaussian noise that occurs naturally in a wireless channel. We later included the AWGN channel as a benchmark for all the rest of the models developed. The Fig 5.1 shows the results of the simulation.

5.1.1 Explanation

The piece of software written corroborates very well with the theoretical probability bit error rate. The result demonstrated the legitimacy of our developed model.

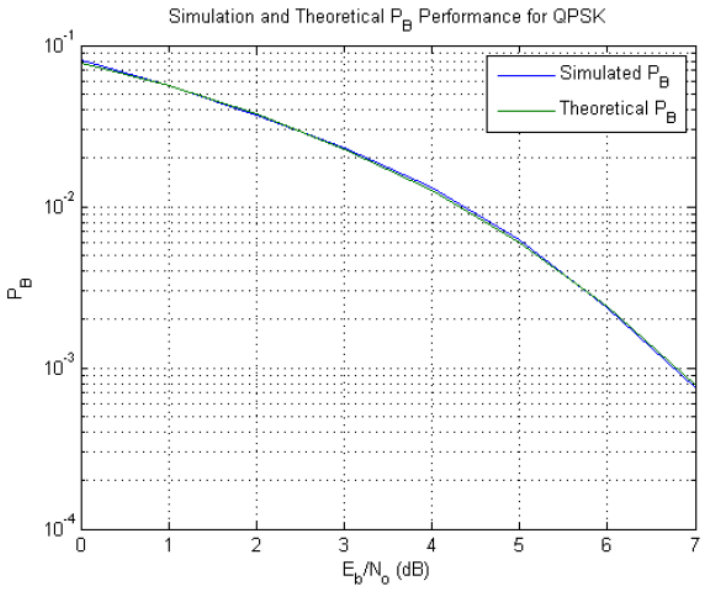

Figure 5.1: QPSK Performance

5.1.2 Challenges

Derivation of noise variance and establishing its relationship to SNR.

5.2 Jakes Flat Fading Time-varying Channel

The Jakes Rayleigh model is a flat fading model, having only one tap in the wideband tapped delay line model. See Fig 5.2 and Fig 5.3 showing the plot results. The data speed is 14,000 bits/sec, transmit frequency of 900 Ghz, mobile receiving station moving at 110km/h which are reasonable parameters for a moving vehicle in an urban area. The simulations ran for a block length of 4096 bits and the number of samples per baud (symbol) was at 16 samples/symbol. To gauge the performance, we used the AWGN channel as a benchmark. As mentioned earlier, the Jakes model assumes that the scatterers are uniformly distributed around a circle at angles α_n with k rays emerging from each scatterer and the Doppler shift on ray n is given as $f_n = f_d \cos \alpha_n$. The model is time-varying as the moving mobile receiving unit experience a Doppler shift. It is flat fading because there is no time dispersion, but only frequency dispersion. As explained in the code in the previous chapter, the model involves generating the Jakes PSD, and obtaining the Jakes filter from that to finally generate the tap gain process (in this case just one), by filtering white gaussian noise through the filter. Fig 5.6 and Fig 5.7 shows the Jakes filter and PSD respectively.

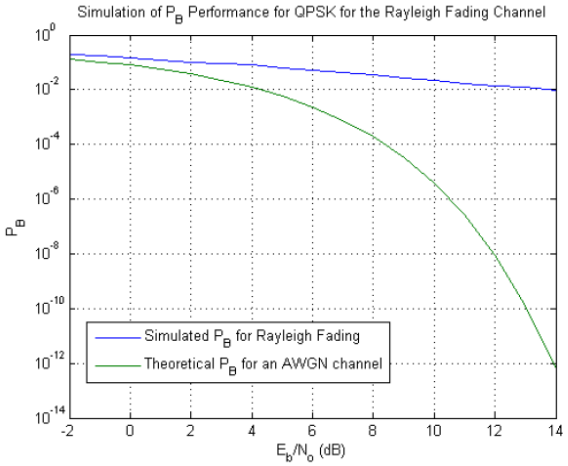

Figure 5.2: Probability Bit error against SNR plot for Jakes flat fading time varying system

5.2.1 Explanation

The plot shows the Rayleigh fading decaying linearly as SNR increases. Quoting Andreas Molisch from his book "Wireless Communications", [39] , in a fading channel, the BER decreases only linearly with the average SNR. The relationship between instantaneous BER and instantaneous SNR is highly non-linear, so that the cases of low SNR essentially determine the overall BER". From the plot, we see that the Rayleigh Fading plot tends to flattens as SNR increases further validating the fact with higher SNR, the probability bit error depends on the probability of deep fades occuring. Looking at the second plot, Fig 5.3, we can see how the fading envelope varies with time. Note the deep fade the signal experiences between 0.06 to 0.08 seconds and this could potentially affect the bit error rate negatively. Note the the performance is worst than the theoretical AWGN channel. One more interesting feature to look at are the imaginary and real components of the QPSK signal shown in Fig 5.4 and Fig 5.5. These plots demonstrate how the signals are fading within the symbol.

5.3 SNR Monitoring Techniques

We came up with two estimators, one suitable for slow Rayleigh fading channels and a moments-based EVB estimator based on the works of Hafez [22] and results on their effectiveness will be shown in the next subsections.

5.3.1 Slow Fading Estimator

As described earlier in the previous chapter, we first derived an estimator (complete derivation in chapter 2) and it was found that it is only suitable for slow Rayleigh fading

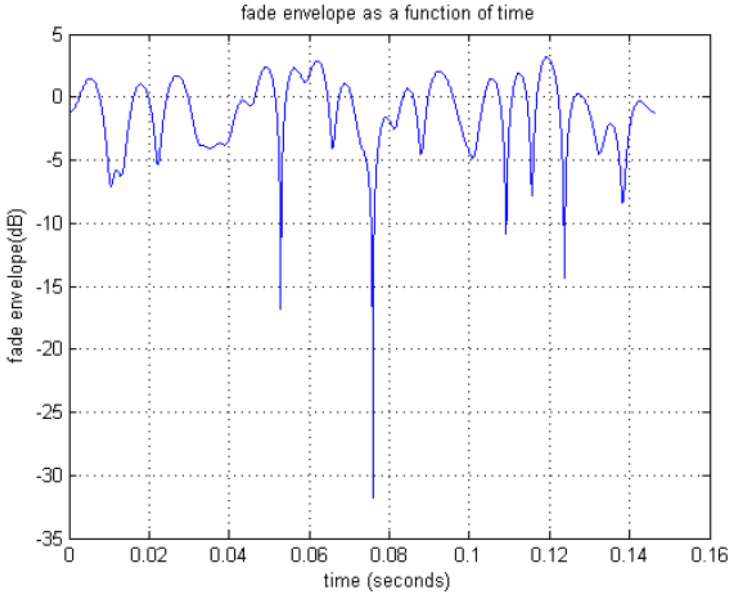

Figure 5.3: Fade envelope of the received signal

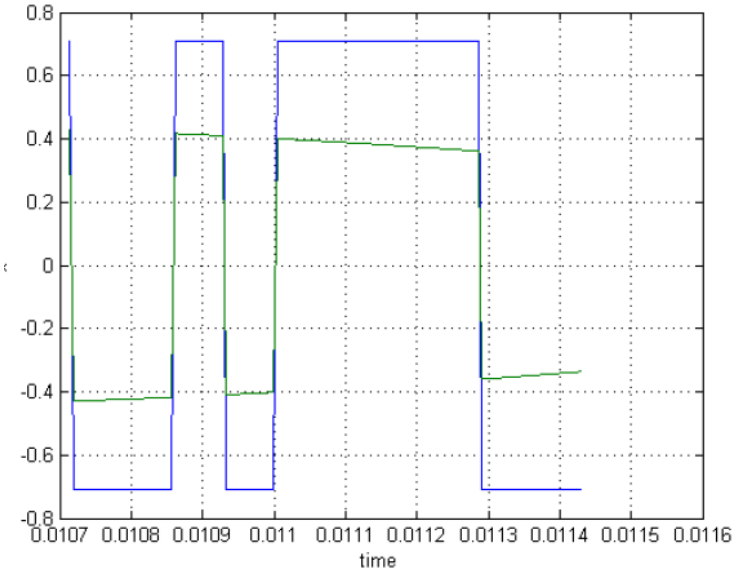

Figure 5.4: Q Component of the QPSK signal

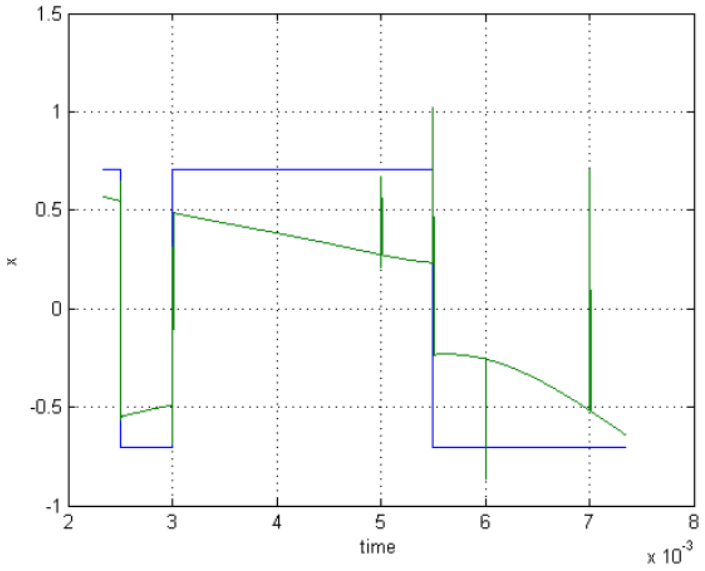

Figure 5.5: I component of the QPSK signal

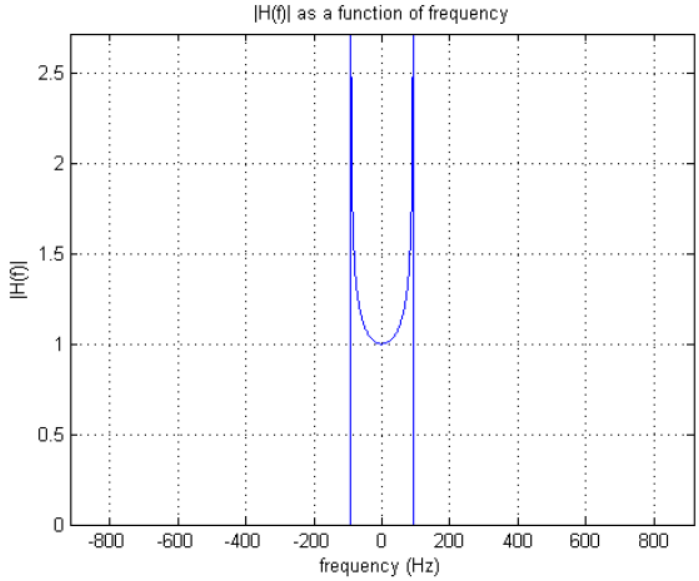

Figure 5.6: Jakes Doppler Filter to produce the tap gain processes

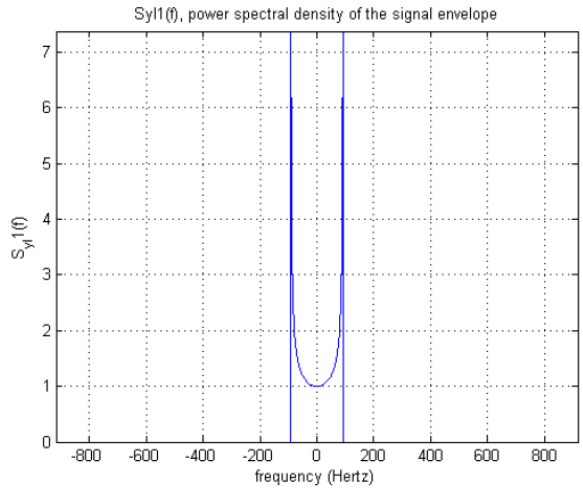

Figure 5.7: The Power Spectral Density of the signall

channels, where the coherence time is greater than the symbol time, that is the fading is constant over a range of symbols. We simulate the adaptive modulation simulation of a mobile cognitive radio user moving at a speed of 25 km per hour, packet size of 36 bits, for 1000 packets, bit rate of 2000 bits per second, which means 18 symbols (QPSK mode), 12 symbols (8PSK mode) and 9 symbols (16PSK) are used in computing the estimate. Modulation schemes are switched based on SNR estimated for each packet. We computed a histogram of the error between the true value and estimated SNR value. The Figure 5.8 below shows that the designed SNR estimator is effective with most values falling near the 0dB discrepancy region, with few errors with minor values of a maximum of around 0.8dB

5.3.2 Challenges

Though fairly direct derivation, this estimator would fail when the packet blocklength has a large value in the order of hundreds, or thousands and the Doppler frequency is high. After some delving into the analytical side of estimator, we realised that, for the estimator to give accurate results, it was important that the following conditions are met:

1. The estimator window size should be comparable size to the block length
2. The coherence time $(1/f_d)$ should be more than the symbol time, that is the fading should be constant over a range of symbols. The estimator would output inaccurate values when there is fast fading within the symbol time.

5.3.3 Moments-based EVB Estimator

This moments-based EVB estimator (complete derivation in chapter 2) was implemented in a fast fading adaptive modulation simulation, where the coherence time $(1/f_d)$ is a lot

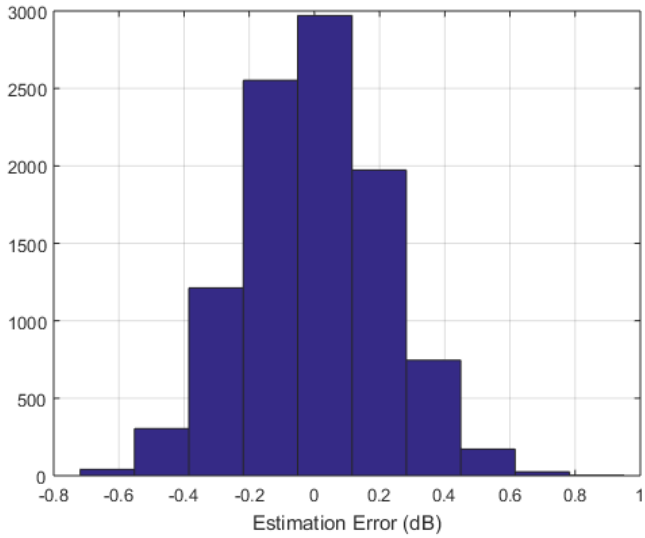

Figure 5.8: SNR Estimator performance (slow fade)

less than the symbol time, that is there is fading within a symbol time. The simulation was ran for a mobile cognitive radio user moving at a speed of 500km/h (very fast fading scenario), doppler frequency, 416.7 Hz a packet length of 12000 bits, which means 6000 symbols (QPSK), 4000 symbols (8PSK) and 3000 symbols (QPSK) and switching modulations based on SNR estimated for each packet.The Figure 5.9 below shows a histogram illustrating the effectiveness of the moment based estimator.

5.3.4 Challenges

This estimator as derived and described in [22] is perfect for this fast fading scenario, however, this estimator has been defined to cater for time domain analysis. Since we were working with complex envelope, we had to work out how to design it for the complex envelope and was successful in doing so as explained in chapter 4, when we treated the real and imaginary parts independently and averaged them to find the estimated SNR. One more important thing to note here is that, in translating it to the frequency domain, we realise, we lost an important faculty, Hafez et al. touted in his paper, which is the fact that the estimator is independent of the signal constellation. Hence we had to work out polynomial fits for the three different modulation schemes to compute an accurate SNR estimate. In contrast to [32], this M2M4 moments estimator was indeed a success in implementation for the M-PSK modulation schemes.

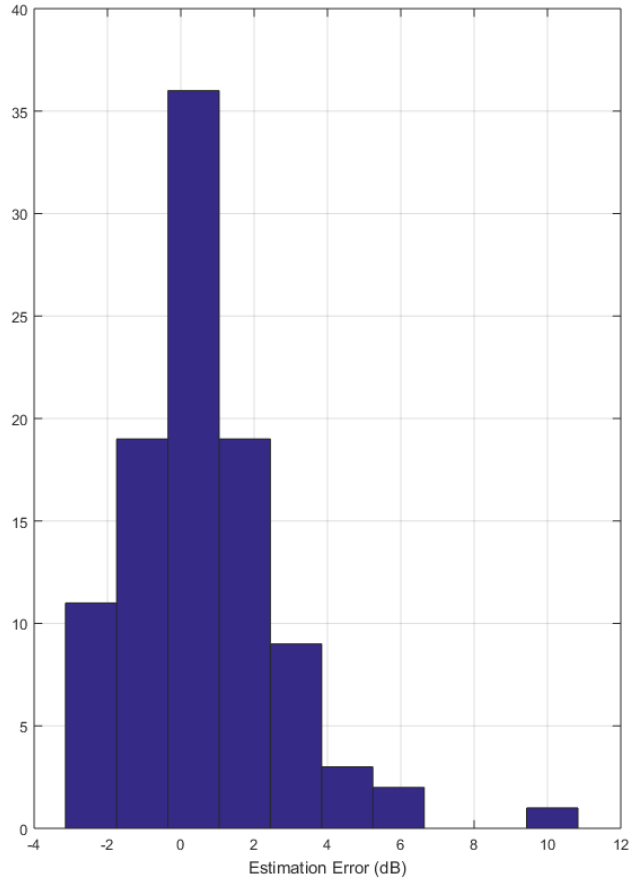

Figure 5.9: M2M4 Moments-based EVB Estimator

5.4 BER Performance Curves Rayleigh Fading Channel

The BER performance curves of QPSK, 8PSK and 16PSK over a flat Rayleigh fading channel is illustrated in Figure 5.10

5.5 Adaptive Modulation Techniques

The adaptive modulation simulation program works as follows: Basically it is a Monte Carlo simulation, which first computes the switching levels, l_n using the falsi method, to obtain the exact breakpoint values from the AWGN theoretical formulae. Then for a fixed blocklength packet, and a fixed number of packets, a complex envelope is generated, then goes through an MPSK modulator, then passed through a Jakes Doppler filter, to finally

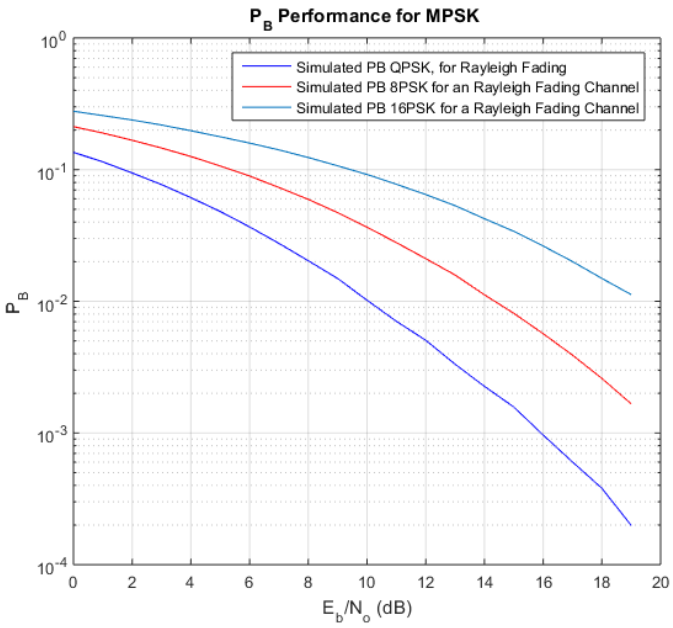

Figure 5.10: MPSK Rayleigh Fading Channel BER Performance

be demodulated and the BER performance is calculated. After demodulation, the SNR value of the received signal is estimated and the next packet in the simulation switches modulation based on the estimated SNR value.

5.5.1 Slow Fading Adaptive Modulation BER Performance

The fig 5.11 below shows the plot of an adaptive modulation BER performance for a slow fading Rayleigh channel. The required BER was set to be 10^{-6}. The breakpoints are apparent in the plot. Based on the switching levels, which are, choose QPSK if the SNR range is: $l \geq 9.5879$, and we choose 8PSK if the SNR range is :$9.5879 < l \leq 14.7955$ and finally we choose 16PSK modulation if the SNR is higher than 14.7955.

Explanation

Broadly speaking the BER curve for the adaptive modulation system shows a clear performance improvement as compared to the 16PSK curve. As the received SNR increases, the system switches to higher order modulation, and in the events of deep fades, the systems switches to the lower order, more robust modulation to maintain the required BER. The advantage of this adaptive system is primarily in the cognitive radio context, bandwidth saving is important and we have to maintain the quality of transmission. In the dynamic environment, the adaptive system enables the CR user to use available bandwidth as they become opportunistically available and transmit at minimum power causing less co-channel interference. As the signal degrades, it have mechanisms to switch

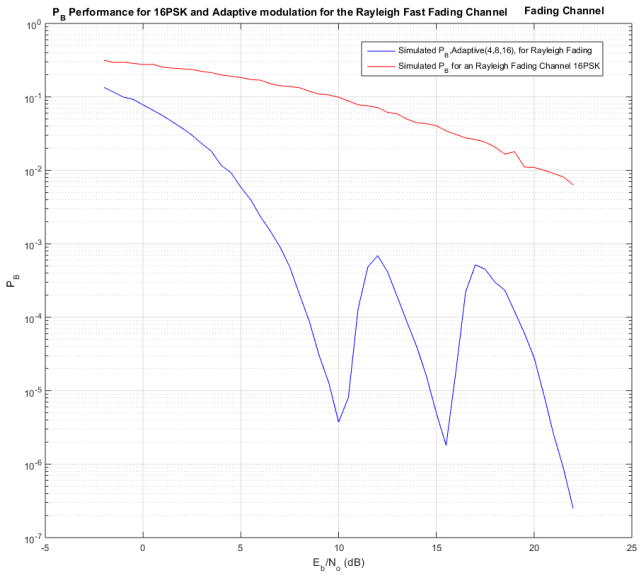

Figure 5.11: Slow Fading Adaptive Modulation

to more robust, though less Bandwidth efficient modulations, to counteract and maintain the required BER.

5.5.2 Fast Fading Rayleigh Channel

The simulation program works as the slow fading one, though we implemented the M2M4 estimator that was able to handle, extreme velocity of 500km/h for example. Interestingly, the M2M4 estimator performs well if the coherence time is less than the symbol time.

Explanation

The Figure 5.12 above shows the relative improvement in performance compared to the 16PSK curve and just like the slow fading scenario, as the SNR increases, the adaptive system switches to higher order modulation which are more spectrally efficient and switches to more robust lower order modulation as SNR degrades to maintain the required BER. More precisely, when there is opportunistic bandwidth availability, the cognitive radio transmitter can use adaptive modulation to transmit at minimum power that meets the BER constraint and data throughput requirements, and in doing so, it minimises co-channel interference between other users in the network and also it uses power and bandwidth efficiently. One interesting point to note in this scenario is that we assumed minimal or no channel delay and perfect channel statistics being relayed to the transmitter through the feedback channel. However, if the channel is fast fading, that puts a strain on the feedback channel and it is of utmost importance that this feedback channel is as reliable as possible, ideally with error correction and coding techniques implemented.

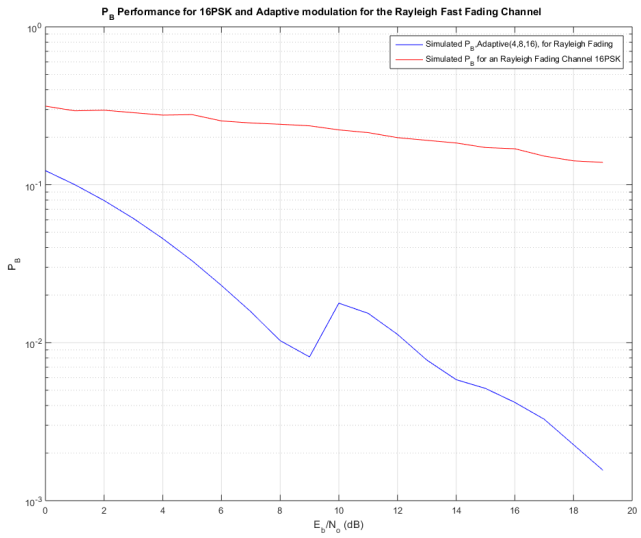

Figure 5.12: Very Fast Fading Adaptive Modulation

5.6 Conclusion

We illustrated performance gain of adaptive modulation using simulation programs, further proving the effectiveness of adaptive techniques. This work can be further extended, by paying special attention to channel delay and relay channel to investigate further the effects of these factors in a very fast fading environment.

Chapter 6

Conclusion

Research in the field of Cognitive Radio have been gaining momentum over the few decades and it has emerged as good potential in solving current wireless communication system problems resulting from limited available spectrum and inefficient spectrum usage. Cognitive Radio's ability to exploit the existing electromagnetic spectrum opportunistically and adapt to a dynamic wireless environment with fading and co-channel interference makes it a plausible communication paradigm.This thesis went through primarily the concept of adaptive modulation and how it can be incorporated in cognitive radio networks to enhance the performance, be it efficient power and bandwidth usage or maintainig an acceptable BER. Simulations devised have shown how switching modulation schemes at the transmitter, based on the SNR estimate relayed back from the receiver, can help wireless systems withstand moderate to very fast fading environment and meet the required BER constraint. Also, in the same breath, cognitive radio, through the use of adaptive modulation can make use of opportunistically available bandwidth while transmitting at minimum power, hence keeping co-channel interference to a minimum. In [21] Goldsmith and Chung pointed out spectral efficiency is relatively insensitive to which degrees of freedom are adapted. They mention how little spectral efficiency is lost when the power or rate is constrained. In this thesis, the rate was constrained and we adapted the modulation scheme, subject to a BER constraint. Since restricting one or two degrees of freedom in adaptive modulation yields close to maximum possible spectral efficiency by utilising all degrees of freedom, therefore the results obtained in chapter 5, mainly 5.11 and 5.12 are tangible and we can more precisely, see that with increasing SNR, the adaptive modulation simulation for both the slow fading and fast fading switched to higher order modulations to maintain the BER constraint. Moreover it was seen that the overall improvement in BER as compared to just using 16PSK modulation as shown in the simulation results.

In addition, the adaptive modulation system proves to be resilient as it switches to lower order and more robust modulation as it experiences deep fades/nulls(see envelope plot in chapter 5), hence the markedly better performance as shown in the Figures 5.11 and 5.12, as SNR increases.On the other hand, since in a cognitive radio scenario, bandwidth availability is opportunistic, once more bandwidth is available the cognitive radio user can

use adaptive modulation to transmit at minimum power that meet the BER constraint and data throughput requirements, hence being both power and bandwidth efficient. In line with the conclusion in , we can translate the improved BER performance in fading channels to also mean that we gain in spectral efficiency as we vary the modulation scheme based on the SNR value. It is clear that as pointed out in [16], [21], a very stable control or feedback channel is mandatory. Understandably in a fast fading environment, a resilient feedback channel with error correction and coding is very important to ensure the transmitter gets relayed the correct information with minimal delay and adapts accordingly. An example of a system which demonstrates the advantage of adaptive modulation is in a two-way VSAT system. It uses received signal quality feedback from remote sites and based on this information, it can increase the outlink modulation depth in clear sky conditions and decrease it during rainy period. Therefore, in favourable conditions a high capacity communication link can be established and in case of extreme heavy rain service can still be maintained by reducing the information rate further. In this case, adaptive modulation allows the VSAT systems to keep successful communications even in bad weather conditions when received signal quality degrades.

In this project, we clearly showed the advantages of adaptive modulation in the context of cognitive radio. Advances can be realised both in throughput efficiency and bandwidth efficiency through the use of adaptive modulation as illustrated in plots Figures 3.2 to 3.7. Techniques to estimate the received signal to noise ratio which enable adaptive modulation have been demonstrated. Finally, the feasibility of the use of adaptive modulation in Cognitive Radio systems has been established in this work.

6.1 Future work

Currently, work is being done in the implementation of LDPC codes and future publications or thesis will analyse the advantage of adaptive modulation and coding in fading environments. Moreover, we aim to investigate and implement new SNR estimators and also to analyse adaptive modulation and coding systems and the effect of channel delays and co-channel interference which were assumed absent for the purpose of this thesis.

Appendix A

Derivation of Noise Variance and Discrete Time Representation of System

To perform a digital simulation, a discrete model as shown in figure A.1. Figure A.1 illustrates the discrete time model for the communication system where $\tilde{s}\,[k]$, $n[k]$, $r[k]$ are the discrete time parameters of $\tilde{s}\,(t)$, $\tilde{n}\,(t)$, $\tilde{r}\,(t)$ respectively, and k is an integer label for discrete time. Note, $s(t)$ is a bandpass continous time signal, $\tilde{s}(t)$ is the complex envelope i.e. complex low pass signal of s(t). Similarly, $\tilde{n}(t)$ is the noise as a complex baseband signal and finally $\tilde{r}(t)$ is the complex envelope of the received signal.

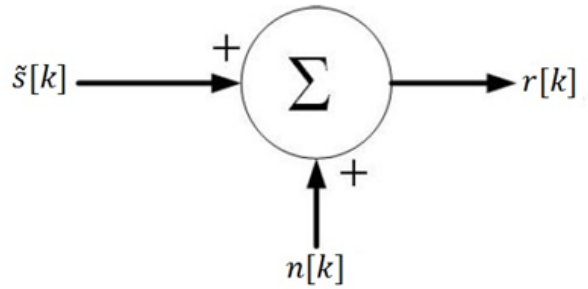

Figure A.1: Discrete time model

In our discrete simulation model, to transmit a symbol, the symbol is divided over discrete time. Consider the rectangular pulse of amplitude A and symbol Time, T_s, shown in Fig below. The symbol time is given by

$$T = N_{SPB}T_S \tag{A.1}$$

Where N_{SPB} is the number of samples per baud or symbol. There will be N_{SPB} samples taken for any one symbol. Using equation derived for Energy of symbol, E_s above, we have the following expression for the energy per symbol. Now, each sample during the simulation will have amplitudes, A, and using equation derived above for the Energy of symbol, E_s, we get the following expression for the energy per symbol

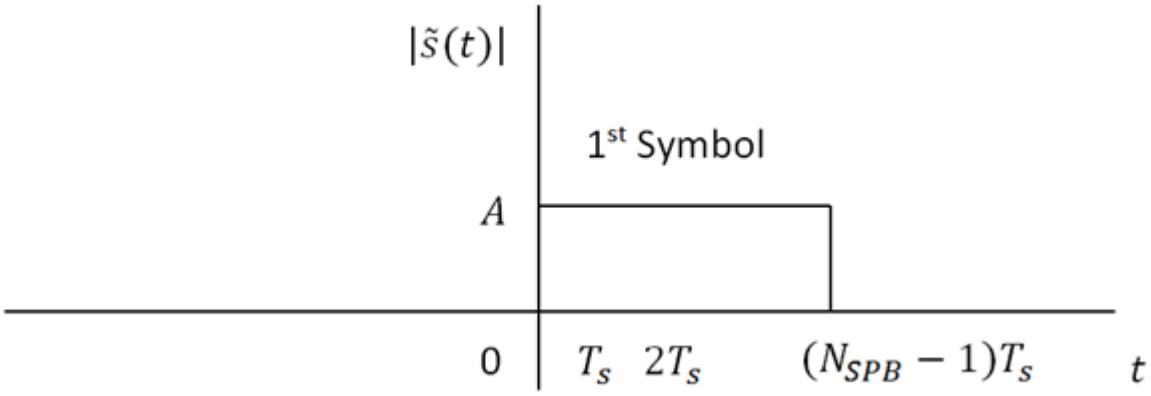

Figure A.2: Sampling of symbol in time

$$E_s = \frac{A^2 T}{2} \tag{A.2}$$

Where E_s is the energy per symbol and T is the time period for a symbol. At this stage, we must now establish relationship between E_b/N_0 and the noise variance $\sigma_{\tilde{n}}^2$. The complex envelope of the noise has a power spectral density of $2N_0$ from -B to B which means that the noise power of each time sample is $2N_0B$. Therefore, the average power is the variance with zero mean random variables and is given by

$$\sigma_{\tilde{n}}^2 = 2N_0B \tag{A.3}$$

By making N_0 the subject of the formula we have

$$N_0 = \frac{\sigma_{\tilde{n}}^2}{2B} \tag{A.4}$$

The energy per symbol is twice the energy per bit i.e. there are two bits per symbol for QPSK

$$E_b = 2E_s = \frac{A^2T}{2} \tag{A.5}$$

Quoting equation for $E_{\tilde{s}}$:

$$E_{\tilde{s}} = \frac{A^2T}{4} \tag{A.6}$$

Substituting (A3) in (A4) yields

$$\frac{E_s}{N_0} = \frac{\frac{A^2}{4}T\,(2B)}{2\sigma_{\tilde{n}}^2} = \frac{A^2TB}{\sigma_{2\tilde{n}}^2} \tag{A.7}$$

We substitute for T by going back to (A1)

$$\frac{2E_b}{N_0} = \frac{E_s}{N_0} = \frac{A^2BN_{SPB}T_s}{\sigma_{2\tilde{n}}^2} \tag{A.8}$$

Making the variance of the random variable the subject of the formula we get

$$\sigma_{\tilde{n}}^2 = \frac{A^2BN_{SPB}T_s}{\frac{4E_b}{N_0}} \tag{A.9}$$

B is the simulation bandwidth affected by noise during the simulation. In line with Shannon's sampling theorem, the sampling frequency should be twice the signal bandwidth. The bandwidth in this case is $\frac{B}{2}$ and hence the sampling frequency is given by:

$$f_s = 2\,(B/2) = B \tag{A.10}$$

Where f_s is the sampling rate. The relationship between f_s and T_s is given by

$$f_s = \frac{1}{T_s} \tag{A.11}$$

Substituting in (A11) gives

$$\sigma_{\tilde{n}}^2 = \frac{A^2\frac{1}{T_s}N_{SPB}T_s}{2\frac{E_b}{N_0}} = \frac{A^2N_{SPB}}{4\frac{E_b}{N_0}} \tag{A.12}$$

Hence establishing the relationship between noise variance $\sigma_{\tilde{n}}^2$ and E_b/N_0.

A.1 Proof Transformation Technique

In this section, we outline the theorem that underlie the result, in equation (3.5).The theorem is the fact that the square of a Rayleigh(α) variable [40] is an exponential(α) random variable and the proof is as follows: Let the random variable, X, have the Rayleigh distribution with probability density function

$$f_X(x) = \frac{2x}{\alpha}\exp(\frac{-x^2}{\alpha}), x > 0 \tag{A.13}$$

for α ¿ 0. The transformation $Y = g(X) = X^2$ is a 1-1 transformation from $X = \{x|x > 0|\}$ to $Y = \{y|y > 0\} with inverse\ X = g^{-1}(Y) = \sqrt(y)$ and Jacobian

$$\frac{dX}{dY} = \frac{1}{2\sqrt(Y)} \tag{A.14}$$

Hence by transformation technique, the probability density function of Y is:

$$f_Y(y) = f_X(g^{-1}(y))|\frac{dx}{dy}|$$

$$= \frac{2\sqrt(y)}{\alpha}\exp(\frac{-\sqrt{y^2}}{\alpha})\left|\frac{1}{2\sqrt{2}}\right|$$

$$f_Y(y) = \frac{1}{\alpha}\exp(\frac{-y}{\alpha}),\ y > 0 \tag{A.15}$$

A.2 16PSK & QPSK transmission power relationship

The K value, linking the QPSK and 16PSK transmission power, was derived as follows: We first look at the probability bit error for QPSK and 16PSK modulation scheme in AWGN channel
for QPSK, the probability of bit error is given by,

$$P_{B,QPSK} = Q\sqrt{\frac{2E_b}{N_o}} = Q\left(\sqrt{\frac{2P_{r,QPSK}}{N_o R_B}}\right). \tag{A.16}$$

For 16PSK, the probability of bit error is given by,

$$P_{B,16PSK} = \frac{2}{\log_2(16)}Q\left(\sqrt{\frac{2E_b\log_2(16)}{N_o}}\sin\left(\frac{\pi}{16}\right)\right) \tag{A.17}$$

$$= \frac{1}{2}Q\left(\sqrt{\frac{8E_b}{N_o}}\sin\left(\frac{\pi}{16}\right)\right) \tag{A.18}$$

$$P_{B,16PSK} = \frac{1}{2}Q\left(\sqrt{\frac{8E_b}{N_o}}\sin\left(\frac{\pi}{16}\right)\right) \tag{A.19}$$

$$P_{B,16PSK} = \frac{1}{2}Q\left(\sqrt{\frac{8P_{r,16PSK}}{N_o R_B}}\sin\left(\frac{\pi}{16}\right)\right) \tag{A.20}$$

where

$$Q(x) = \frac{1}{\sqrt{(2\pi)}}\int_x^\infty \exp\left(\frac{-y^2}{2}\right)dy, \tag{A.21}$$

For

$$P_{B,QPSK} = P_{B,16PSK}, \tag{A.22}$$

Using the approximation,

$$Q(x) \approx \frac{1}{2}\exp\left(\frac{-x^2}{2}\right), \tag{A.23}$$

$$\frac{1}{2}\exp\left(-\frac{P_{r,QPSK}}{N_0 R_B}\right) = \frac{1}{4}\exp\left(-\frac{4P_{r,16PSK}}{N_0}\right)\sin^2\left(\frac{\pi}{16}\right) \tag{A.24}$$

Therefore

$$\frac{P_{r,QPSK}}{N_0 R_B} = \log_e(2) + \frac{4P_{r,16PSK}}{N_0}\sin^2\left(\frac{\pi}{16}\right) \tag{A.25}$$

For sufficiently large $\frac{P_{r,QPSK}}{N_0 R_B}$,

$$\frac{P_{r,QPSK}}{N_0 R_B} \approx \frac{4P_{r,16PSK}}{N_0 R_B}\sin^2\left(\frac{\pi}{16}\right) \tag{A.26}$$

$$P_{r,QPSK} \approx 4P_{r,16PSK}\sin^2\left(\frac{\pi}{16}\right) \tag{A.27}$$

$$\frac{P_{r,QPSK}}{4\sin^2(\frac{\pi}{16})} \approx P_{r,16PSK} \tag{A.28}$$

$$6.5685P_{r,QPSK} \approx P_{r,16PSK} \tag{A.29}$$

$K = 6.5685$ is the constant of proportionality linking the QPSK and 16PSK received powers for the same bit error rate.

A.3 Proof Sequential Channels available

This equation feature in [41] and can be proved as such:

Given

$$N_p(\alpha,\beta,d)=\sum_{j=0}^{min\{\frac{\alpha}{d+1},\beta\}}(-1)^j\binom{\beta}{j}\binom{\alpha-j(d+1)+\beta-1}{\beta-1} \tag{A.30}$$

For an urn model, the number of ways of distributing α identical balls into β identical cells with limited capacity d. Let M be the number of N bit binary words with k ones such that there are at least two adjacent ones in the word, Then,

$$M=\binom{N}{k}-N_p(k,n-k+1,1)$$

$$M=\frac{N!}{k!(N-k)!}-\sum_{j=0}^{min\{\frac{k}{2},n-k+1\}}(-1)^j\binom{N-k+1}{j}\binom{N-2j}{N-k} \tag{A.31}$$

Where, $[x]$, is the largest integer small or equal to x. The analytical solution was proven by counting binary words with adjacent pairs of ones in a MATLAB program which yielded identical solution.

Appendix B

MATLAB source code

B.1 Jakes Doppler Filter

```
function [y,phase_y,Power_ave_measured]=envelope_Jakes(M,Power,fD,fs)

sigma_y=sqrt(Power);
if fs<4.*fD
    fprintf('Aliasing:  The sampling rate is too small')
else
    x(1:M)=(1/sqrt(2))*(randn(1,M)+j.*randn(1,M));
    x(M+1:2*M-1)=zeros(1,M-1);
    X=fft(x);
    M1=2*M-1;
    Ix=[0:1:M/2-1];
    for i=1:length(Ix)
        if Ix(i).*fs./(M1*fD)>=1
            Ix(i)=0;
            H(i)=0;
        else
            H(i)=sqrt(1./sqrt(1-(Ix(i).*fs./(M1.*fD)).^2));
        end
    end
    Iy(2.*M-M/2:2*M-1)=[-M./2:1:-1];
    for i=2*M-M/2:2*M-1
        if abs(Iy(i).*fs./(M1.*fD))>=1
            H(i)=0;
        else
            H(i)=sqrt(1./sqrt(1-(Iy(i).*fs./(M1.*fD)).^2));
        end
    end
    H(M/2:2*M-M/2)=0;
```

```
    H=H.*sigma_y./sqrt(pi*fD./fs);
    Z=H.*X;
    z=ifft(Z);
    y(1:M)=abs(z(1:M));
    phase_y(1:M)=phase(z(1:M));
    Power_ave_measured=mean(y.*(y));
end
```

B.2 Adaptive modulation in a Rayleigh Fading Channel

```
clear
clc

counter_8PSK = 0;
counter_16PSK = 0;
counter_QPSK = 0;

% estimating parameters

c_zero = 10971.3670508672;
c_one = -64731.6367893422;
c_two = 143212.237224577;
c_three = -140825.801468004;
c_four = 51938.6459401357;
% cubic

b_zero = -1566.0419834643;
b_one = 6973.4026101590;
b_two = -10357.0288229892;
b_three = 5131.6668286643;

 P_16PSK_r =   [1498.718405331193
   -14668.068263213330
    53785.989547609468
   -87599.051319916776
    53482.790139211982];

P_16PSK_i = [1506.960836962091
```

```
   -14749.782417356562
    54089.472127732777
   -88099.463736928432
    53791.863303070000];

P_8PSK_r =  [1533.021242314440
   -15004.871033012392
    55023.551850599571
   -89615.889902277690
    54712.742220862099];

P_8PSK_i = [1532.694023475766
   -14996.648361125126
    54975.642431258922
   -89510.160175190336
    54632.134484819937];


P_QPSK_r = [50.189436437983
     -158.794599373812
      180.665362089899
      -76.736202203745
       10.984481300060];

P_QPSK_i =  [50.189436437983
     -158.794599373812
      180.665362089899
      -76.736202203745
       10.984481300060];

  P_r = P_QPSK_r;
  P_i = P_QPSK_i;

Eb_No_dB= [0:1:19];

% size_packet=6000; % bits
% size_packet=24*16*24; %bits
size_packet=6000; %bits
N_packets=100; % number of packets simulated
A=1; % signal amplitude
Nspb= 16; % number of samples per baud
M=16;
v_km_hr= 200;% v_km_hr is the velocity in km/hr
```

```
v=v_km_hr*1000/3600; % v is the velocityt in m/sec
fo=900.e6; % fo is the transmit frequency in Hertz
c=3.e8; % c is the speed of light in m/sec
fD=v*fo/c; % fD is the Doppler frequency in Hertz
Rb=1e3; % Rb is the bit rate in bits/s
fs=Rb*Nspb./2; %fs is the sample rate in samples/s
PbReq = 10e-6;
%_____________________________________________
Eb_No=10.^(Eb_No_dB./10);

NobitsPerSymbol = log2(M);
N_symbols_per_block = size_packet/NobitsPerSymbol;
N_samples=Nspb*N_symbols_per_block; %number of samples in a packet
blocklength = size_packet;

N = 100; % number of errors

% falsi method to find breakpoints

x =arcQfunc(PbReq,.00000001);
Eb_No_dB_QPSK = 10*log10(.5*x*x)

y = arcQfunc(1.5*PbReq,0.0000001);
Eb_No_dB_8PSK = 10*log10((1.5*y*y)/(sin(pi/3)))

z =  arcQfunc(2*PbReq,0.0000001);
Eb_No_dB_16PSK = 10*log10((2*z*z)/(sin(pi/4)))

for iEbNo=1:length(Eb_No_dB);
    sigma=abs(A)*sqrt(Nspb)/(2*sqrt(Eb_No(iEbNo)));
    condition = 0;
    N_errors = 0;
    N_bits = 0;
    while condition == 0

        for n=1:N_packets

            %         H = zeros(1,N_samples);
            %         H = jakesFilter(fs,fD,N_samples);
            [y,phase_y,Power_ave_measured]=envelope_Jakes(N_samples,1,fD,fs);

            % Scale to unity average power in the Fade
            n_fade_env=y./sqrt(Power_ave_measured);
```

```
    eta=sigma.*(randn(1,N_samples)+j.*randn(1,N_samples));
    data = zeros(size_packet);
    data=round(rand(1,size_packet));

    %%%%%%%%%%%%%%%%%%%%%%%%%%%%%%%%%%%%%%%%%%%%%%%%%%%%

data1 = reshape(data,NobitsPerSymbol,blocklength/NobitsPerSymbol);
jval = (0:M-1)';
mapping = bitxor(jval,bitshift(jval,-1));
bitmap=deci2bin(mapping',NobitsPerSymbol);
symbolmapping=[(0:M-1)' bitmap];
si = exp(j.*2.*pi./M.*(0:M-1)');

for iPhase = 1:size(si)

    siPhases(iPhase) = atan2(imag(si(iPhase)),real(si(iPhase)));
    siPhasesOne(iPhase) = siPhases(iPhase);
    if siPhases(iPhase) < 0
        siPhases(iPhase) = siPhases(iPhase) + 2*pi;
    end
    if siPhases(iPhase) == 0
        siPhasesOne(iPhase) = 2*pi;
    end
end

% use the random data generated and check each set of symbols and
% maps them on the constellation diagram.

s=zeros(1,length(data1));
sd=zeros(1,length(data1)); % stores symbols in decimal label format
for counter=1:size(data1,2),
    mData=data1(1:NobitsPerSymbol,counter)';
    for counter2=1:M,
        if mData== symbolmapping(counter2,2:end),
            sd(counter)=symbolmapping(counter2,1);
            s(counter)=exp(j.*2.*pi./M.*symbolmapping(counter2,1));
        end
    end
end

    %%%%%%%%%%%%%%%%%%%%%%%%%%%%%%%%%%%%%%%%%%%%%%%%%%%%

    x = zeros(1,N_samples);
```

```
for ii=1:size_packet/NobitsPerSymbol  %Generate signal vector for the
    x((ii-1)*Nspb+1:(ii*Nspb))=s(ii).*ones(1,Nspb);
end
for k=1:N_samples
    freq(k)=(-N_samples/2-1+k)*fs./N_samples;
end

for kk=1:N_samples
    x(kk)=x(kk).*n_fade_env(kk);  % Fading on the signal
 % x(kk)=x(kk);% No signal fading
end

y=x+eta;
           % calculate the number of bits
N_bits = N_bits + blocklength;
iir = 0;
for ii=1:blocklength/NobitsPerSymbol   % Symbol detection
    u=real(sum(y((ii-1)*Nspb+1:(ii*Nspb))));
    v=imag(sum(y((ii-1)*Nspb+1:(ii*Nspb))));

    % ****** sum of R over Nspb *********
    R(ii) = (1/Nspb)*(sum(y((ii-1)*Nspb+1:(ii*Nspb))));

    Sym_detected_phase = atan2(v,u);

    if Sym_detected_phase < 0
        Sym_detected_phase = Sym_detected_phase + 2*pi;
    end

    Sym_detected_phase = mod(Sym_detected_phase,2*pi);
    [c index] = min(abs(siPhases - Sym_detected_phase));
    [d index1] = min(abs(siPhasesOne - Sym_detected_phase));

    if c < d
        detectedSymbol = symbolmapping(index,2:end);
    else
        detectedSymbol = symbolmapping(index1,2:end);
    end

    for iiter = 1:NobitsPerSymbol
        datar(iiter+iir) = detectedSymbol(iiter);
    end
    iir = iir + NobitsPerSymbol;
```

```
          end


          % Hafez et al. Estimator implementation

          Eb_No_dB(iEbNo)

  z_numerator =.5*mean(abs(real(R)).*abs(real(R)))+...
  .5*mean(abs(imag(R)).*abs(imag(R)))
z_denominator = .5*(mean(abs(real(R)).*(abs(real(R)))+...
.*(abs(real(R))).*(abs(real(R)))))^2 +...
.5*(mean(abs(imag(R)).*abs(imag(R)).*abs(imag(R)).*abs(imag(R))))^2
        m_two_r =  mean((abs(real(R))).^2);
        m_four_r = mean((abs(real(R))).^4);

        m_two_i =  mean((abs(imag(R))).^2);
        m_four_i = mean((abs(imag(R))).^4);

         real_R = abs(real(R));
         imag_R = abs(imag(R));

        z_hat_qpsk = z_numerator./(z_denominator)
        z_hat_r = m_four_r./((m_two_r).^2)
        z_hat_i = m_four_i./((m_two_i).^2)


        if M == 4

         z_hat_real(iEbNo,n)=z_hat_qpsk;
         z_hat_ave_real(iEbNo)=mean(z_hat_real(iEbNo,:))

           z_hat_imag(iEbNo,n)=z_hat_qpsk;
         z_hat_ave_imag(iEbNo)=mean(z_hat_imag(iEbNo,:))

         z_hat_r = z_hat_qpsk;
         z_hat_i = z_hat_qpsk;

        else

         z_hat_real(iEbNo,n)=z_hat_r;
        z_hat_ave_real(iEbNo)=mean(z_hat_real(iEbNo,:))
```

```
        z_hat_imag(iEbNo,n)=z_hat_i;
        z_hat_ave_imag(iEbNo)=mean(z_hat_imag(iEbNo,:))

       end

  gamma_m = 2;
  Eb_No_est_dB_r(iEbNo)=P_r(1).*z_hat_r.^4 +...
  P_r(2).*z_hat_r.^3+P_r(3).*z_hat_r.^2 +...
  P_r(4).*z_hat_r +P_r(5);
  Eb_No_est_dB_i(iEbNo)=P_i(1).*z_hat_i.^4 +P_i(2).*z_hat_i.^3...
+P_i(3).*z_hat_i.^2 + P_i(4).*z_hat_i +P_i(5);
   Eb_No_est_dB(iEbNo) = (Eb_No_est_dB_r(iEbNo) + Eb_No_est_dB_i(iEbNo))./2


        Error(iEbNo)=100*(Eb_No_dB(iEbNo)-Eb_No_est_dB(iEbNo))/Eb_No_dB(iEbNo
        dB_diff(iEbNo,n)= Eb_No_est_dB(iEbNo)-Eb_No_dB(iEbNo);

        fprintf('Eb_No_dB=%16.8f,...
        Eb_No_est_dB=%16.8f\n',Eb_No_dB(iEbNo),Eb_No_est_dB(iEbNo))
         mean_eb(iEbNo,n) = Eb_No_est_dB(iEbNo);
         Eb_est_ave(iEbNo) = mean(mean_eb(iEbNo,:));

         errornumber=sum(mod((data(1:blocklength)+datar(1:blocklength)),2));
        % Number of bit errors in block
        N_errors=N_errors+errornumber;

        if Eb_No_est_dB(iEbNo) < (Eb_No_dB_QPSK)
           fprintf('changed to 4psk')
            M =16;
            NobitsPerSymbol = log2(M);
            N_symbols_per_block = size_packet/NobitsPerSymbol;
            %number of samples in a packet
            N_samples=Nspb*N_symbols_per_block;
            blocklength = size_packet;
            P_r = P_8PSK_r;
            P_i = P_8PSK_i;
            counter_QPSK = counter_QPSK + 1;
        else if Eb_No_est_dB(iEbNo) >= (Eb_No_dB_QPSK) &&...
        Eb_est_ave(iEbNo) < (Eb_No_dB_8PSK)
               fprintf('changed to 8psk')
                M =16;
            NobitsPerSymbol = log2(M);
                N_symbols_per_block = size_packet/NobitsPerSymbol;
```

```
                    %number of samples in a packet
                    N_samples=Nspb*N_symbols_per_block;
                    blocklength = size_packet;
                    P_r = P_8PSK_r;
                    P_i = P_8PSK_i;
                    counter_8PSK = counter_8PSK + 1;

                else if Eb_No_est_dB(iEbNo) >= (Eb_No_dB_8PSK)
                        fprintf('changed to 16psk')
                        M = 16;
                        NobitsPerSymbol = log2(M);
                        N_symbols_per_block = size_packet/NobitsPerSymbol;
                        %number of samples in a packet
                        N_samples=Nspb*N_symbols_per_block;
                        blocklength = size_packet;
                         P_r = P_8PSK_r;
                         P_i = P_8PSK_i;
                        counter_16PSK = counter_16PSK + 1;
                    end
                end
            end

            blocklength
            size(R)
            ii
            clearvars s sd siPhases siPhasesOne symbolmapping counter R...
            z_hat_i zhat_r m_two_i m_two_r m_four_i m_four_r

        end
                % Total Number of bit errors
        if N_errors>N    % Condition to terminate the simulation
            condition=1;
        end

        PB(iEbNo)=N_errors/N_bits; % bit error rate estimate
        fprintf('Eb/No=%14.2f dB,

    end
 end

PB_Q = [0.135421666666667 0.114506666666667 0.0943033333333333...
0.0769900000000000 0.0612583333333333 0.0481100000000000...
0.0367200000000000 0.0275283333333333 0.0203083333333333...
```

```
0.0149000000000000 0.0101883333333333 0.00704666666666667...
0.00505666666666667 0.00332666666666667 0.00226000000000000...
0.00157333333333333 0.000963333333333333 0.000601666666666667...
0.000380000000000000 0.000198333333333333];

PB_8= [0.212126666666667 0.189665000000000 0.167116666666667
0.145955000000000 0.125810000000000 0.106620000000000...
0.0894200000000000 0.0731750000000000 0.0594350000000000 0.0471183333333333
0.0365483333333333 0.0279000000000000 0.0210866666666667...
0.0158300000000000 0.0111983333333333 0.00810333333333333...
0.00567333333333333 0.00389833333333333 0.00259500000000000...
0.00166166666666667];

PB_16 = [0.277668333333333 0.257450000000000 0.238291666666667...
0.218313333333333 0.197530000000000 0.177750000000000...
0.159118333333333 0.141275000000000 0.123625000000000...
0.106911666666667 0.0918450000000000 0.0773966666666667...
0.0646900000000000 0.0532466666666667 0.0424150000000000...
0.0339883333333333 0.0262833333333333 0.0200383333333333...
0.0149166666666667 0.0112300000000000];


figure(1)
semilogy(Eb_No_dB,PB_Q,'b',Eb_No_dB,PB_8,'r',Eb_No_dB,PB_16)
grid
xlabel('E_b/N_o (dB)')
ylabel('P_B')
title('P_B Performance for MPSK ')
legend('Simulated PB QPSK, for Rayleigh Fading',...
    'Simulated PB 8PSK for an Rayleigh Fading Channel',...
    'Simulated PB 16PSK for a Rayleigh Fading Channel')% 'R =
for i=1:length(Eb_No_dB);
    average(i)=mean(dB_diff(i,:))
    sd(i)=std(dB_diff(i,:))
    maximum(i)=max(abs(dB_diff(i,:)))
end
figure(2)
plot(Eb_No_dB,average,'r',Eb_No_dB,sd,'b',Eb_No_dB,maximum,'g')
grid
xlabel('E_b/N_o (dB)')
ylabel('Estimation Error (dB)')
title('E_b/N_o Estimation')
legend('mean','standard deviation','peak absolute')
```

```
figure(3)
hist(dB_diff(11,:))
xlabel('Estimation Error (dB)')
grid
```

Bibliography

[1] "Cisco visual networking index: Global mobile data traffic forecast update 2014-2019 white paper," 2014.

[2] E. Docket, "Spectrum policy task force report," vol. 41, pp. 48–52, March.

[3] J. et al, "Cognitive radio: Making software radios more personal," vol. 6, pp. 13–18, August 1999.

[4] S. Mao, *Video over Cognitive Radio Networks*. Springer, 2014.

[5] Y. H. Chye, E. Dutkiewicz, R. Vesilo, and R. P. Liu, "Adaptive spectrum sensing for cognitive radio systems in a fading environment," in *Wireless Personal Multimedia Communications (WPMC), 2014 International Symposium on*, pp. 451–456, Sept 2014.

[6] R. Pfeifer, C. Scheier, and I. Illustrator-Follath, *Understanding intelligence*. MIT press, 2001.

[7] S. Haykin, "Cognitive radio: brain-empowered wireless communications," *Selected Areas in Communications, IEEE Journal on*, vol. 23, no. 2, pp. 201–220, 2005.

[8] D. Cabric, S. Mishra, and R. Brodersen, "Implementation issues in spectrum sensing for cognitive radios," in *Signals, Systems and Computers, 2004. Conference Record of the Thirty-Eighth Asilomar Conference on*, vol. 1, pp. 772–776 Vol.1, Nov 2004.

[9] R. V. Prasad, P. Pawelczak, J. Hoffmeyer, H. S. Berger, *et al.*, "Cognitive functionality in next generation wireless networks: standardization efforts," *Communications Magazine, IEEE*, vol. 46, no. 4, pp. 72–78, 2008.

[10] M.-S. Alouini and A. J. Goldsmith, "Adaptive modulation over nakagami fading channels," *Wireless Personal Communications*, vol. 13, no. 1-2, pp. 119–143, 2000.

[11] J. K. Cavers, "Variable-rate transmission for rayleigh fading channels," *Communications, IEEE Transactions on*, vol. 20, pp. 15–22, Feb 1972.

[12] T. Ue, S. Sampei, and N. Morinaga, "Symbol rate and modulation level controlled adaptive modulation/tdma/tdd for personal communication systems," in *Vehicular Technology Conference, 1995 IEEE 45th*, vol. 1, pp. 306–310 vol.1, Jul 1995.

[13] W. Webb and R. Steele, "Variable rate qam for mobile radio," *Communications, IEEE Transactions on*, vol. 43, pp. 2223–2230, Jul 1995.

[14] A. Goldsmith and S.-G. Chua, "Variable-rate variable-power mqam for fading channels," *Communications, IEEE Transactions on*, vol. 45, pp. 1218–1230, Oct 1997.

[15] H. Matsuoka, S. Sampei, N. Morinaga, and Y. Kamio, "Adaptive modulation system with variable coding rate concatenated code for high quality multi-media communication systems," in *Vehicular Technology Conference, 1996. Mobile Technology for the Human Race., IEEE 46th*, vol. 1, pp. 487–491 vol.1, Apr 1996.

[16] M.-S. Alouini, X. Tang, and A. J. Goldsmith, "An adaptive modulation scheme for simultaneous voice and data transmission over fading channels," *Selected Areas in Communications, IEEE Journal on*, vol. 17, no. 5, pp. 837–850, 1999.

[17] M. Barnela, "Digital modulation schemes employed in wireless communication: A literature review," *International Journal of Wired and Wireless Communications*, vol. 2, no. 2, pp. 15–21, 2014.

[18] A. Goldsmith, *Wireless Communications*. Cambridge University Press, 2005.

[19] J. Torrance and L. Hanzo, "Adaptive modulation in a slow rayleigh fading channel," 1996.

[20] Y. Kamio, S. Sampei, H. Sasaoka, and N. Morinaga, "Performance of modulation-level-controlled adaptive-modulation under limited transmission delay time for land mobile communications," in *Vehicular Technology Conference, 1995 IEEE 45th*, vol. 1, pp. 221–225 vol.1, Jul 1995.

[21] S. T. Chung and A. J. Goldsmith, "Degrees of freedom in adaptive modulation: a unified view," *Communications, IEEE Transactions on*, vol. 49, no. 9, pp. 1561–1571, 2001.

[22] M. Hafez, T. Khattab, and H. Shalaby, "Blind snr estimation of gaussian-distributed signals in nakagami fading channels," *Wireless Communications, IEEE Transactions on*, vol. 14, pp. 3509–3518, July 2015.

[23] M. Fujii and Y. Watanabe, "A study on snr estimation for cognitive radio," in *Ultra-Wideband (ICUWB), 2012 IEEE International Conference on*, pp. 11–15, IEEE, 2012.

[24] H. Al-Hmood, R. Abbas, A. Masrub, and H. Al-Raweshidy, "An estimation of primary user's snr for spectrum sensing in cognitive radios," in *Innovative Computing Technology (INTECH), 2013 Third International Conference on*, pp. 479–484, Aug 2013.

[25] S. Sharma, S. Chatzinotas, and B. Ottersten, "Snr estimation for multi-dimensional cognitive receiver under correlated channel/noise," *Wireless Communications, IEEE Transactions on*, vol. 12, pp. 6392–6405, December 2013.

[26] K. Seshukumar, R. Saravanan, and M. Suraj, "Spectrum sensing review in cognitive radio," in *Emerging Trends in VLSI, Embedded System, Nano Electronics and Telecommunication System (ICEVENT), 2013 International Conference on*, pp. 1–4, Jan 2013.

[27] F. Bellili, A. Stephenne, and S. Affes, "Snr estimation of qam-modulated transmissions over time-varying simo channels," in *Wireless Communication Systems. 2008. ISWCS '08. IEEE International Symposium on*, pp. 199–203, Oct 2008.

[28] D. Pauluzzi and N. Beaulieu, "A comparison of snr estimation techniques for the awgn channel," *Communications, IEEE Transactions on*, vol. 48, pp. 1681–1691, Oct 2000.

[29] A. Das, "Nda snr estimation: Crlbs and em based estimators," in *TENCON 2008-2008 IEEE Region 10 Conference*, pp. 1–6, IEEE, 2008.

[30] A. Ramesh, A. Chockaligam, and L. B. Milstein, "Snr estimation in generalized fading channels and its application to turbo decoding," in *Communications, 2001. ICC 2001. IEEE International Conference on*, vol. 4, pp. 1094–1098, IEEE, 2001.

[31] A. Ramesh, A. Chockalingam, and L. B. Milstein, "Snr estimation in nakagami-m fading with diversity combining and its application to turbo decoding," *Communications, IEEE Transactions on*, vol. 50, no. 11, pp. 1719–1724, 2002.

[32] S. Dianat, "Snr estimation in nakagami fading channels with arbitrary constellation," in *Acoustics, Speech and Signal Processing, 2007. ICASSP 2007. IEEE International Conference on*, vol. 2, pp. II–325–II–328, April 2007.

[33] S. M. Kay, "Fundamentals of statistical signal processing: Detection theory, vol. 2," 1998.

[34] F. Beukers, "Gauss hypergeometric function," in *Arithmetic and geometry around hypergeometric functions*, pp. 23–42, Springer, 2007.

[35] A. Abdi and M. Kaveh, "Performance comparison of three different estimators for the nakagami m parameter using monte carlo simulation," *Communications Letters, IEEE*, vol. 4, no. 4, pp. 119–121, 2000.

[36] E. C. Y. Peh, Y. C. Liang, Y. L. Guan, and Y. Zeng, "Power control in opportunistic spectrum access cognitive radio with sensing information at transmitter," in *Communications (ICC), 2011 IEEE International Conference on*, pp. 1–5, June 2011.

[37] B. Sklar, *Digital communications*, vol. 2. Prentice Hall NJ, 2001.

[38] R. Ziemer and W. H. Tranter, *Principles Of Communications: System Modulation And Noise*. John Wiley & Sons, 2006.

[39] A. F. Molisch, *Wireless communications*. John Wiley & Sons, 2007.

[40] P. Shankar, *Fading and Shadowing in Wireless Systems*. SpringerLink : Bücher, Springer New York, 2011.

[41] N. Balakrishnan and M. Koutras, *Runs and Scans with Applications*. Wiley Series in Probability and Statistics, Wiley, 2011.